Climate Change and Cleaner Emissions Decrease Methylmercury Export from a Headwater Peatland Catchment

Colin McCarter[1], Stephen D Sebestyen[2], Jeff D. Jeremiason[3], E.A. Nater[4], and Randy Kolka[2]

[1]Nipissing University
[2]USDA Forest Service
[3]Gustavus Adolphus College
[4]U Minnesota

July 27, 2023

Abstract

Peatlands are sources of the bioaccumulating neurotoxin methylmercury (MeHg) and linked to adverse health outcomes, yet the impact of climate change and reductions in atmospheric pollutants on mercury (Hg) export from peatlands are highly uncertain. Here, we present the response in annual flow-weighted concentrations (FWC) and yields of total-Hg (THg) and MeHg to cleaner air and climate change using an unprecedented hydroclimatic (55-years; streamflow, air temperature, precipitation, regional and peatland water tables), depositional chemistry (21-years; Hg and major ions concentration and total mass), and streamwater chemistry (˜17-years; THg, MeHg, major ions, total organic carbon, and pH) datasets from a reference peatland catchment in the north central USA. Over the hydroclimatic record, annual mean air temperature increased by ˜1.8 , decreasing baseflow and, subsequently, the efficiency that precipitation was converted to streamwater runoff (runoff ratio). Concurrently, precipitation-based deposition of sulfate and Hg declined, where wet Hg deposition rates declined to near pre-industrial levels. Annual MeHg FWC was positively correlated mean annual air temperatures ($p=0.03$, $r=0.51$), annual runoff ratio ($p<0.0001$, $r=0.76$), and wet Hg deposition concentration ($p<0.0001$, $r=0.79$). Over the study period, decreasing wet Hg deposition concentration and annual runoff ratios counterbalanced increased peatland MeHg production due to higher air temperatures, leading to an overall decline in streamwater MeHg FWC. Climate change and cleaner air were responsible for 0.51 and 0.32 of the variability in MeHg FWC, respectively. Streamwater MeHg export may continue to decrease only if declines in runoff ratio and wet Hg deposition concentration persistently outpace increased air temperature.

Hosted file

968705_0_art_file_11205772_ry25y6.docx available at https://authorea.com/users/643316/articles/656738-climate-change-and-cleaner-emissions-decrease-methylmercury-export-from-a-headwater-peatland-catchment

Climate Change and Cleaner Emissions Decrease Methylmercury Export from a Headwater Peatland Catchment

C.P.R. McCarter[1], S.D. Sebestyen[2], J.D. Jeremiason[3], E.A. Nater[4], R.K. Kolka[2]

[1] Department of Biology and Chemistry & Department of Geography, Nipissing University; 100 College Drive, North Bay, Ontario, Canada

[2] USDA Forest Service Northern Research Station, Grand Rapids, Minnesota 55744, USA

[3] Department of Chemistry, Gustavus Adolphus College, 800 W College Ave St. Peter, MN 56082, USA

[4] Department of Soil, Water, and Climate, University of Minnesota, St. Paul, Minnesota 55108, USA

Corresponding author: Colin McCarter (colinmcc@nipissingu.ca)

Key Points:

- Lower annual streamwater methylmercury concentrations due to compounding effects of climate change and cleaner air
- Higher mean annual air temperature increases annual streamwater methylmercury
- Lower wet atmospheric mercury deposition and runoff ratio offset higher air temperatures, resulting in lower methylmermcury concentrations

Abstract

Peatlands are sources of the bioaccumulating neurotoxin methylmercury (MeHg) and linked to adverse health outcomes, yet the impact of climate change and reductions in atmospheric pollutants on mercury (Hg) export from peatlands are highly uncertain. Here, we present the response in annual flow-weighted concentrations (FWC) and yields of total-Hg (THg) and MeHg to cleaner air and climate change using an unprecedented hydroclimatic (55-years; streamflow, air temperature, precipitation, regional and peatland water tables), depositional chemistry (21-years; Hg and major ions concentration and total mass), and streamwater chemistry (~17-years; THg, MeHg, major ions, total organic carbon, and pH) datasets from a reference peatland catchment in the north central USA. Over the hydroclimatic record, annual mean air temperature increased by ~1.8 ℃, decreasing baseflow and, subsequently, the efficiency that precipitation was converted to streamwater runoff (runoff ratio). Concurrently, precipitation-based deposition of sulfate and Hg declined, where wet Hg deposition rates declined to near pre-industrial levels. Annual MeHg FWC was positively correlated mean annual air temperatures ($p=0.03$, $r=0.51$), annual runoff ratio ($p<0.0001$, $r=0.76$), and wet Hg deposition concentration ($p<0.0001$, $r=0.79$). Over the study period, decreasing wet Hg deposition concentration and annual runoff ratios counterbalanced increased peatland MeHg production due to higher air temperatures, leading to an overall decline in streamwater MeHg FWC. Climate change and cleaner air were responsible for 0.51 and 0.32 of the variability in MeHg FWC, respectively. Streamwater MeHg export may continue to decrease only if declines in runoff ratio and wet Hg deposition concentration persistently outpace increased air temperature.

Plain Language Summary

Climate change and cleaner air are unequivocally altering mercury cycling in a headwater stream fed by a peatland-rich catchment. Using long-term and broad environmental measurements we

45 show that decreasing stream methylmercury is due to lower annual mean wet mercury deposition
46 concentration and annual runoff ratios, which offsets potential increases of methylmercury from
47 elevated mean annual air temperatures. As such, methylmercury export from headwater peatland
48 catchments will continue to decrease over time if climate change continues to accelerate the
49 reduction of runoff ratios and atmospheric wet mercury deposition further decreases. To better
50 adapt to future climate and environmental change, there is a need for more and longer integrated
51 multidisciplinary datasets. Without these long-term and integrated measures these critical
52 insights would not have been possible.

53

1 Introduction

Climate change is altering stream and river water chemistry (Li et al., 2022; Meyer-Jacob et al., 2019). In boreal and hemi-boreal catchments, wetlands, including peatlands, play a critical role in regulating water chemistry (Gorham et al., 1985; Lam et al., 2022; Schelker et al., 2014), particularly the contaminant mercury (Hg) (Kronberg et al., 2018; Lam et al., 2022; Mitchell et al., 2008b; Tjerngren et al., 2012a). Yet, other concurrent environmental disturbances potentially compound or mask changes in water chemistry from climate change (Li et al., 2021). Even in ecosystems that are assumed to be least impacted and that serve as reference sites, decreased atmospheric deposition of pollutants, such as sulfate (SO_4^{2-}) or Hg, with cleaner air legislation (Lee et al., 1998; Pannatier et al., 2011; Sickles II & Shadwick, 2015; Zhang et al., 2019) may mask or enhance effects of climate change on aqueous contaminants like Hg. Untangling relative effects of climate and environmental change in reference ecosystems is critical to inform science, management, and policy.

The bioaccumulating neurotoxin methylmercury (MeHg) is a contaminant of global concern linked to adverse human health conditions (O'Connor et al., 2019). Mercury mobilization, either as MeHg or total-Hg (THg), from uplands and wetlands to downstream water bodies is controlled by interacting hydrological and biogeochemical processes that affect both concentrations and fluxes (Bishop et al., 2020; Branfireun et al., 2020; McCarter et al., 2022b; O'Connor et al., 2019; Woerndle et al., 2018). Peatlands are often sources of MeHg to surface waters (Branfireun et al., 1998; Lam et al., 2022; Skyllberg et al., 2003; Woerndle et al., 2018). The net export of MeHg from peatlands to surface waters is a balance between Hg methylation and demethylation(Kronberg et al., 2018; Tjerngren et al., 2012b), MeHg solubility (Skyllberg, 2008), and the hydrological transport of Hg from a peatland to a stream (McCarter et

al., 2022b). In peatlands, wet atmospheric Hg deposition is usually lower than dry Hg deposition but is often more readily available to resident microbial communities (Hsu-Kim et al., 2013), likely resulting in quicker incorporation into the peatland Hg cycle. Elevated atmospheric SO_4^{2-} deposition to peatlands has been linked to increased MeHg concentrations in receiving streamwater (Jeremiason et al., 2006; McCarter et al., 2022b) but the effect is rapidly reversible once SO_4^{2-} additions decline (Coleman Wasik et al., 2012; McCarter et al., 2017; McCarter et al., 2022b). While both SO_4^{2-} and Hg deposition have decreased in response to clean air legislation, climate change likely affects the ecohydrological and biogeochemical process that underpin Hg cycling and export (Bishop et al., 2020; Yang et al., 2016). Model simulations of the effect of climate change on Hg cycling are unclear due to large uncertainties associated with both climate change and Hg biogeochemical processes (Golden et al., 2013), while *in-situ* experimental warming of boreal peatlands have shown increases in both inorganic Hg and MeHg porewater concentrations (Sun et al., 2023). However, few long-term empirical datasets exist to document contemporary responses and trends, particularly at catchment scales. Correspondingly, the response in Hg export from peatlands due to the long-term and interacting effects of climate change and cleaner air is uncertain (Sonke et al., 2023), largely due to only a few select places with sustained, routine Hg monitoring in streamwater in conjunction with relevant environmental data collection.

We present an unprecedented 17-year record of annual flow-weighted concentrations (FWC) of THg and MeHg and frame that record within longer 55-year hydroclimatic and ~30-year atmospheric deposition records for Hg and basic chemistry. Combined, we used these datasets to quantify directionality and magnitude of responses and to discern mechanisms that

govern Hg concentrations and yields in a headwater hemi-boreal stream. Data were collected within the long-term ecosystem research program of the USDA Forest Service at the S2 catchment on the Marcell Experimental Forest (MEF) in Minnesota. As far as we are aware, the dataset is the only multi-decadal, uninterrupted record for boreal or hemi-boreal streamwater MeHg and THg. The hydroclimatic record consists of the annual mean, minimum, and maximum air temperature, total precipitation, catchment runoff, baseflow/event flow contributions, and the fraction of precipitation that occurs as streamflow (runoff ratio) (Sebestyen et al., 2021). Atmospheric deposition records include the Hg concentration, total mass of wet Hg deposition, and total wet-deposited mass of nitrate, SO_4^{2-}, hydrogen ion, sodium, and chloride (National Atmospheric Deposition Program (MN16), 2020, 2021). Streamwater chemistry samples were taken 8 to 24 times a year, when water was flowing, and analyzed for THg, MeHg, total organic carbon (TOC) and major anions and cations (Sebestyen et al., 2022). Our findings are the first catchment-scale observations that show how both THg and MeHg export from peatland-dominated catchments change with interacting effects of cleaner air and climate change.

2 Study Site

The S2 catchment has served as a minimally disturbed reference catchment at the MEF since the 1960s (Sebestyen et al., 2011). The MEF is located in north-central Minnesota with a continental climate and average daily temperature of 3.5 °C and annual precipitation of ~787 mm (Sebestyen et al., 2021). The 9.7 ha catchment is comprised of a 6.5 ha upland that surrounds a centrally located 3.2 ha forested ombrotrophic bog peatland (Sebestyen et al., 2021). The bog peatland has an overstory of chiefly *Picea mariana* and an understory of *Sphagnum* mosses, graminoids, and ericaceous shrubs (Verry & Janssens, 2011). The upper ~30 cm of peat is

derived from the current forested bog vegetation and transitions from poor fen to rich fen peat deeper through the peat profile (Verry & Janssens, 2011). The peat depth is from 10s of cm to ~7 m (Verry & Janssens, 2011). The uplands are dominated by a mixed deciduous forest of *Populus tremuloides* with other coniferous and deciduous tree (Verry & Janssens, 2011).

The peatland and upland both hydrologically feed a lagg that surrounds the peatland, which ultimately drains into a small stream (Sebestyen et al., 2011; Verry et al., 2011). The ombrotrophic bog peatland and surrounding uplands are perched above the regional aquifer, isolating deep groundwater contributions from both the uplands and peatland (Verry et al., 2011). Consequently, the uplands provide local groundwater to the lagg and peatland through relatively shallow permeable loess sandy loam horizon overlying a low-permeability Koochiching clay loam till (Mitchell et al., 2009; Verry et al., 2011). The water flow at the catchment stream outlet is monitored at a v-notch weir (Verry et al., 2018).

3 Methods

All the data and associated QA/QC used in this study are from freely accessible data publications and aggregated to annual and/or seasonal values for analysis (Table 1), as well as additional QA/QC analysis is presented McCarter et al. (2022b) and the associated supplemental information. The collated dataset included water chemistry (including major ions, TOC, and Hg measured at least every 1 to 2 weeks when there was streamflow), atmospheric deposition (SO_4^{2-}, pH, ions, and Hg), total daily precipitation amount, mean (and min/max) daily air temperature, daily streamflow, daily peatland water table elevation, and monthly water table elevation in the aquifer adjacent to the peatland catchment, and calculated runoff ratios (*RR*), daily baseflow/event flow, proportion event flow, potential evapotranspiration (PET), and the 10-year average PET (Table 1).

148 **Table 1.** Data sources for the different measured parameters, with measurement frequency and
149 the calculations used for each parameter.

150

Data Source	Parameters	Measurement Frequency	Calculations
Sebestyen et al. (2021)	Streamflow, air temperature, precipitation, regional and peatland water tables	Daily (1962-2017)	All Parameters: Annual and seasonal means, standard deviations, and deviations from long-term mean (1962-1972); event flow and baseflow, proportion of baseflow/event flow; annual and seasonal total precipitation (P); Annual and seasonal runoff ratio, standard deviation of annual runoff ratio (calculated using monthly data); Annual mean potential evapotranspiration (PET), Annual and 10-year mean potential evapotranspiration P-PET
Sebestyen et al. (2022)	THg, MeHg, K^+, Na^+, Ca^{2+}, Mg^{2+}, $Fe^{2/3+}$, Cl^-, SO_4^{2-}, PO_4^{3-}, pH, TOC	~bi-weekly (1998-2017, 9-24 samples per year)	MeHg/THg: annual and seasonal FWC and yields, standard error of FWC and yields; Cations/anions/pH/TOC: annual FWC and yields
National Atmospheric Deposition Program (MN16) (2021)	Total wet Hg deposition, precipitation wet Hg deposition concentration	Monthly (1996-2017)	Seasonal and annual totals, means, and standard deviation
National Atmospheric Deposition Program (MN16) (2020)	Precipitation concentration of: SO_4^{2-}, Cl^-, NH_4^+, NO_3^-, Br^-, K^+, Na^+, Ca^{2+}, Mg^{2+}, pH	Monthly (1978-2017)	Annual and seasonal means

151

152 *3.1 Data Calculations*

153 Solute yields were calculated following Sebestyen and Kyllander (2017), whereby
154 concentrations were linearly interpolated between water chemistry samples. Daily yield was
155 calculated by multiplying the sample concentration or interpolated concentration by daily
156 streamflow. Daily yields were either seasonally or annually summed (Sebestyen & Kyllander,
157 2017). The seasonal or annual yields were then divided by catchment area (9.7 ha) and the total
158 volumetric streamflow to determine the annual FWC (Sebestyen & Kyllander, 2017). Seasons
159 were defined as: Spring: March-May, Summer: June-August, Fall: September-November,
160 Winter: December-February.

161

162 The 95% confidence intervals for annual MeHg FWC and yields were determined
163 following Hope et al. (1997). The 95% confidence interval of the monthly FWC, $var(C_F)$, were
164 determined using,

$$var(C_F) = \left[\sum (C_i - C_F)^2 \cdot \frac{Q_i}{Q_n}\right] \sum \frac{Q_i^2}{Q_n^2} \quad \text{Eq. 1}$$

165 where, C_F is the monthly FWC for a given solute, C_i is the instantaneous concentration for a
166 given sample, Q_i is the instantaneous discharge, and Q_n is the sum of Q_i. The 95% confidence
167 interval of the yields were then determined by,

$$std.error(Y) = F \cdot \sqrt{var(C_F)} \quad \text{Eq. 2}$$

168 where, F is the total monthly discharge.

169

170 Wet deposition of most solutes and total deposition of Hg were measured as part of the
171 National Atmospheric Deposition Program (NADP). The NADP site is in the Marcell
172 Experimental Forest about 2 km from the S2 catchment.

173

174 Streamflow was separated into base and event flow following Nathan and McMahon (1990),
175 with a recession coefficient of 0.8. Runoff ratios were calculated by,

$$RR = \frac{Q_s}{P} \quad \text{Eq. 3}$$

176 where, Q_s is the annual total streamflow (mm), and P is the annual total precipitation (mm) for a
177 given time period.

178

179 Calculated daily potential evapotranspiration (mm) was determined following Hargreaves and
180 Samani (1985),

$$PET = 0.0023 \cdot 0.408 \cdot R_a\left(T_{avg} + 17.8\right)(T_{max} - T_{min})^{0.5} \quad \text{Eq. 4}$$

181 where, R_a is the extra-terrestrial solar radiation (mm H_2O m^{-2} day^{-1}), T_{avg} is the average daily
182 temperature (°C), T_{max} is the maximum daily temperature (°C), and T_{min} is the minimum daily
183 temperature (°C).
184
185 *3.2 Statistical Analysis*
186 Unless otherwise stated, all statistical analysis was performed in R Statistical Software (R
187 Development Core Team, 2021). All daily values were then averaged to seasonal or annual
188 scales for comparison to the annual MeHg or THg FWC and yields. The annual Hg FWCs and
189 annual Hg yields were first compared to all 118 variables using a Pearson correlation matrix with
190 hierarchical clustering (Wei & Simko, 2017) to identify potential controls on either THg or
191 MeHg. Variables with significant moderate correlations ($R^2 > 0.5$, $p > 0.05$) were identified and
192 the initial 118 variables were reduced by removing temporal co-variates (*i.e.*, annual and
193 seasonal measures) and choosing annual values over seasonal values. However, in some
194 instances it was not immediately clear which co-variate should be removed and, in those cases,
195 both were kept for further analysis (*i.e.*, annual and summer average air temperature). This
196 procedure resulted in a total of seven, eight, three, and six variables for annual MeHg FWC,
197 annual MeHg yield, annual THg FWC, and annual THg yield, respectively.
198
199 Despite reducing the number of potential governing variables, these variables were likely
200 correlated to each other and necessitate further reduction before error in variable linear

regression. Hierarchical partitioning of R^2 with the *hier.part* package (Walsh & Mac Nally, 2020) was used to assess the relative importance of these independent variables on annual Hg FWC and yield. The independent variables (potential drivers) were scaled to the mean and unit variance equal to 0, and the proportion of variance that could be explained by a given independent variable was determined from 999 randomized data matrix using the *rand.hp* function in *heir.part*. Significance ($p < 0.05$) was assessed by the upper confidence 95% confidence interval (Z-score ≥ 1.65) (Mac Nally, 2002; Walsh & Mac Nally, 2020). Hierarchical partitioning determines the proportion of independent and joint variances explained by each variable, allowing for the identification of variables with strong independent correlation with the dependent variable (Chevan & Sutherland, 1991; Mac Nally, 2000), in this case either annual Hg FWC or yield. As such, variables with high correlations but with little independent effect due to joint correlations with other variables would not be significant and were excluded from further analysis.

The remaining significant variables from the hierarchical partitioning analysis were used as the independent variables in individual bivariate linear regressions. However, since both independent and dependent variables vary throughout each year, Deming regression was calculated in SigmaPlot 12.0©. Deming regression is a form of error in variable orthogonal regression that accounts for the standard deviation of the dependent and independent variables at each data point (Deming, 1943). Following York (1966) and Wu and Yu (2018), Deming regression minimizes the sum of squares (*SS*) residuals in both independent and dependent variable by,

$$SS = \sum_{i=1}^{N} [\omega(X_i)(x_i - X_i)^2 + \omega(Y_i)(y_i - Y_i)^2] \quad \text{Eq. 5}$$

where, X_i is the measured driving variable (*e.g.*, mean annual temperature), Y_i is the measured Hg FWC or yields, x_i is the regressed driving variable, and y_i is the regressed Hg FWC or yields. The individual Hg FWC or yields and driving variable were weighted based on annual variability in X_i and Y_i, respectively, following,

$$\omega(X_i) = \frac{1}{\sigma_{X_i}^2}, \omega(Y_i) = \frac{1}{\sigma_{Y_i}^2} \quad \text{Eq. 6}$$

where, σ_{Xi} and σ_{Yi} are the annual standard deviation of X_i and Y_i, respectively. See Wu and Yu (2018) for a detailed comparison of Deming regression to other error in variable linear regression techniques. The error of the independent variables was taken as the standard deviation around the annual mean of a given driver. By using Demming regression rather than other linear regression techniques, we are better able to account for the natural variability in annual measures, which provides a clearer picture of the critical factors controlling Hg dynamics under changing atmospheric conditions.

4 Results and Discussion

There was considerable inter-annual variability in THg FWC but no trend (τ = -0.07, p =0.71, Figure 1, Table S1). Without considering the intra-annual variability in THg FWC, spring runoff ratio was suggested to correlate with THg FWC (Table S2). However, when considering the intra-annual viability in spring runoff ratio and THg FWC, the correlation breaks down at higher THg FWC (Figure 2). As such, none of our measured hydroclimatic variables strongly drive THg FWC, while THg yields (Figure 3, Table S1) were correlated with THg FWC (Figure 2, Table S3). Despite no apparent effect of climate change on THg at annual time-scales, changes

in other unmeasured or time-lagged mechanisms will likely induce shifts in THg fluxes (McCarter et al., 2022a; McCarter et al., 2021a), such as experimental evidence that warmer temperatures increase peatland inorganic Hg pore water concentrations from enhanced microbial activity (Sun et al., 2023). As such, there is an urgent need for more careful consideration and study of the interacting processes that influence THg mobilization to aquatic ecosystems.

Throughout the study period, MeHg FWC varied independently of THg FWC, suggesting disconnects between THg and MeHg transport and cycling processes (Figure 1). Methylmercury FWC decreased (τ = -0.356, p = 0.07) over the 17-year streamwater Hg record from the highest annual MeHg FWC in 2001 and 2002 to the lowest annual concentrations in 2009 and 2013 (Figure 1, Table S1). The proportion of THg as MeHg (%MeHg) significantly decreased (τ = -0.452, p = 0.02) over the 17-year study, paralleling the decrease in MeHg FWC (Figure 1). The observed decrease in both MeHg FWC and yields (Figure 3) could not be ascribed to a single change in climate, streamwater chemistry, or atmospheric deposition metric. A combination of declines in annual wet Hg deposition concentration (23.8%) and the runoff ratio (20.4%), and an increase in mean annual air temperature (22.8%) explains 67% of the independent variability in annual MeHg FWC (Table S4). In contrast, the decline in annual MeHg FWC (32.2%) and annual runoff ratio (16.2%) were the only significant drivers for MeHg yield, accounting for 48.4% of the independent variability but this value increases to 60.5% when including annual streamflow (Table S5). Thus, changes in MeHg FWC, along with climate-controlled streamflow measures (*e.g.*, declines in baseflow or runoff ratios), govern the total mass of MeHg leaving the catchment to downstream aquatic ecosystems. Interestingly, no streamwater chemistry parameters, including TOC and sulfate, were correlated with MeHg FWC or yields. It is important to note that in both cases, THg and MeHg, the yields were strongly dependent on the

FWCs, suggesting that monitoring a larger number of streamwater MeHg concentration may be more an impactful action to assess MeHg impacts than fewer streams with both yields and FWCs.

4.1 Cleaner Air

Sulfur dioxide emissions and subsequent SO_4^{2-} deposition have decreased following clean air legislation first introduced in the 1970s and amended through the 1990s (O'Meara, 1998; Pannatier et al., 2011; Sickles II & Shadwick, 2015). The decline in SO_4^{2-} deposition primarily occurred from the 1970s-1990s, decreasing from 28 kg ha^{-1} yr^{-1} in 1979 to 10 kg ha^{-1} yr^{-1} in 1999 (National Atmospheric Deposition Program (MN16), 2020). During the 2001-2017 streamwater Hg record, annual SO_4^{2-} deposition steadily declined from ~10 to ~4 μg SO_4^{2-} m^{-2} (Figure 3). We expected that atmospheric SO_4^{2-} deposition would be a strong predictor of annual MeHg FWC due to the partial dependence of Hg methylation on microbial SO_4^{2-} reduction in peatlands (Mitchell et al., 2008a; Pierce et al., 2022). However, there was no correlation between SO_4^{2-} deposition and annual MeHg FWC in the outflowing streamwater (Figure S4). Given the large store of sulfur in the surficial peat to buffer these lower SO_4^{2-} inputs (Urban et al., 1989), it is likely that the relative change in SO_4^{2-} deposition during the Hg measurement period was small in relation to the total peat sulfur pool that would allow a detectable change in annual MeHg FWC at the catchment scale from increased Hg methylation (Åkerblom et al., 2013; Mitchell et al., 2008a; Pierce et al., 2022) or solubility (Skyllberg, 2008). As such, current SO_4^{2-} deposition rates are not controlling streamwater MeHg as would have been during past higher SO_4^{2-} deposition rates that stimulate elevated streamwater MeHg (McCarter et al., 2022b) prior to clean air legislation.

290

291 Annual wet Hg deposition at the MEF, first measured during 1996, declined from a peak
292 in 1999 of 10,000 ng Hg m^{-2} to between 6000 to 7000 ng Hg m^{-2} during the 2010s (Figure 4),
293 approaching pre-industrial deposition rates (Li et al., 2020). While wet Hg deposition
294 concentration varied between 9.5 and 14.6 ng L^{-1} (total range 5.1 ng L^{-1}) over the study period
295 (Figure 4). Wet Hg deposition concentration (Figure 4) was positively correlated ($p < 0.0001$, $r =$
296 0.79) with the annual MeHg FWC (Figure 5). Despite dry Hg deposition (e.g., litter fall) being
297 the largest atmospheric Hg input at the MEF (Woerndle et al., 2018), its mobility and availability
298 is often limited relative to wet Hg deposition as additional decomposition or surface erosion
299 processes are often required before impacting streamwater Hg concentrations or yields (Bishop
300 et al., 2020; Demers et al., 2007). As such, given the annual timescales investigated here, recent
301 wet Hg deposition would likely be more bioavailable to the resident methylating microbiota than
302 both legacy Hg that has been bound to organic matter (Chiasson-Gould et al., 2014; Gorski et al.,
303 2008; Hintelmann et al., 2002; Hsu-Kim et al., 2013) and dry Hg deposition, where availability
304 to methylating bacteria may lag well beyond one year. In this case, the decline in the wet Hg
305 deposition explained the greatest amount of variability in the annual MeHg FWC (Figure S2,
306 Table S4), suggesting that further reduction in global atmospheric Hg emissions and subsequent
307 deposition would have a substantial and rapid impact in reducing MeHg in northern peatland
308 catchments. However, given the current deposition concentrations are approaching pre-industrial
309 levels at the MEF, future decreases in wet Hg deposition concentrations may lessen its
310 importance relative to other drivers in this region.

311

312 *4.2 Climate Change*

Climate change is readily apparent at the MEF (Figure 4). From 1962 to 2017, annual mean air temperature significantly increased by ~1.8 ℃, with no trend in precipitation amount (Figure 4). Mean annual air temperature was positively correlated (1.8 ± 1.2 nmol L^{-1} $℃^{-1}$) with annual MeHg FWC (Figure 5). However, over the Hg sampling period, there was no increase in annual mean air temperature (τ = -0.26, p = 0.12), unlike the clear increase from 1961 to 2017 (p = 0.003, Figure 4). In general, mercury methylation is expected to increase with higher microbial activity at warmer air temperatures (Hsu-Kim et al., 2013; Sun et al., 2023; Yang et al., 2016). Such an increase in microbial activity is thought to be more important in the shoulder seasons (spring and fall) where the average air temperatures are further from optimal microbial activity temperatures (IPCC, 2021). However, at annual scales, neither shoulder season mean, minimum, or maximum air temperatures were strong predictors of annual MeHg FWC. Here, warmer mean summertime air temperatures were positively correlated with annual MeHg FWC (Figure S2, Table S2) suggesting that warmer summers combined with *in situ* increases in SO_4^{2-} and changes in water table (Sun et al., 2023) will likely produce higher MeHg FWC. Importantly, these results suggest that annual MeHg FWC responds to mean annual temperature and that future climate warming may have an immediate impact on MeHg concentrations in peatland-fed streamwaters.

In peatlands, other microbially mediated processes, such as heterotrophic respiration or methanogenesis, are sensitive to the timing and magnitude of temperature and water table anomalies but may be temporally limited and masked by using annual means (Feng et al., 2020; Helbig et al., 2022). In the S2 peatland, the seasonal peatland water tables have been disproportionally decreasing due to climate change during the drier summer (-0.0021 ± 0.0008 m

336 yr^{-1}, $p < 0.0001$) and fall (-0.0020 ± 0.0014 m yr^{-1}, $p = 0.005$) periods relative to the wetter
337 spring (-0.0015 ± 0.0009 m yr^{-1}, $p = 0.002$). Here, annual MeHg FWC was positively correlated
338 ($p < 0.05$) with the variability in the annual minimum temperature (defined as one standard
339 deviation of the mean minimum temperature; Figure S1). This increase in temperature variability
340 would likely increase the lower limit of temperature limitations on Hg methylation rates, while
341 lower water tables increase the oxidative production of SO_4^{2-} (Sun et al., 2023). These processes
342 are likely to increase future MeHg concentrations in peatlands (Sun et al., 2023). However,
343 higher soil temperatures can increase gaseous sulfur losses from peatlands that can suppress pore
344 water MeHg concentrations and partially offset the aforementioned increases in MeHg
345 concentrations (Åkerblom et al., 2013). Our results suggest that in isolation further increases in
346 air temperature and variability due to climate change, MeHg concentrations in peatland-fed
347 streams, rivers, and lakes will increase due to this positive feedback.
348
349 In general, higher air temperatures increase evapotranspiration losses (Dymond et al.,
350 2014; Helbig et al., 2020), lowering available soil water in the uplands and decreasing peatland
351 water tables, thus converting less precipitation to stream runoff. Higher evapotranspiration
352 combined with steady precipitation drove a significant decline in baseflow ($\tau = -0.25$, $p = 0.008$),
353 streamflow ($\tau = -0.15$, $p = 0.1$), the amount of precipitation that became streamflow (runoff ratio,
354 $\tau = -0.224$, $p = 0.02$), and an increase in the proportion of event flow ($\tau = 0.321$, $p < 0.001$),
355 particularly since 2000 (Figure 4 and Figure S1). Seasonally, the decline in annual runoff ratio
356 was driven by a significant decrease in fall ($\tau = -0.203$, $p = 0.03$), while both the spring ($\tau = -$
357 0.134, $p = 0.15$) and summer ($\tau = -0.102$, $p = 0.28$) did not significantly decline during the same
358 period (Figure S2). Such declines in runoff ratio due to decreasing baseflow and increases in air

359 temperature that drove higher evapotranspiration is consistent with observations at MEF
360 (Dymond et al., 2014) and projections of climate change (Reshmidevi et al., 2018; Zhang et al.,
361 2023). Despite potential increases in hydrological connectivity between the stream and the
362 catchment during wet periods such as the spring freshet (Jones et al., 2023; Woerndle et al.,
363 2018), the decline in annual runoff ratio is driven by lower water tables during dry periods that
364 offsets any increases in hydrological connectivity during wet periods at annual time scales,
365 driving an overall decrease in the hydrological connectivity of uplands and the peatland to the
366 stream at annual time scales. Thus, precipitation that falls on the catchment is less likely to be
367 transported to the stream during more frequent drier periods (summer and fall).
368
369 The flow and pathways that water moves through a catchment, in short the hydrology, is
370 key to regulating downstream aquatic Hg concentrations and cycling (Branfireun et al., 2020) but
371 the mechanisms are often confounded by other landscape features such as ecosystem types or
372 disturbances (Lam et al., 2022). At the MEF, there has been a clear climate change induced
373 decrease in runoff ratio that decreased overall catchment hydrological connectivity. As such,
374 climate warming has reduced the annual runoff ratio, significantly decreasing annual MeHg
375 FWC and yields (Figure 5). With a 10% decline in annual runoff ratio, which is the approximate
376 average decline over the hydroclimatic record, annual MeHg FWC declined by 2.1 ± 0.6 nmol L^{-1}
377 and yields by 0.001 ± 0.0003 mg ha^{-1}. While no seasonal change in hydrology, upland or
378 peatland, correlated with annual MeHg FWC, peatland water table (*i.e.*, catchment water storage)
379 plays a critical role in facilitating water and solute transport, where higher water tables increase
380 solute transport rates (McCarter & Price, 2017). With the decline in peatland water tables due to
381 climate change, it takes longer and more precipitation for the catchment to hydrologically

reconnect and transport any MeHg produced in the catchment to the streams and increases likelihood of chemical or microbial demethylation (Barkay & Gu, 2022). At the S2 catchment, photodemethylation would likely be limited due to the stream often being dry for extended durations during summer rather than stagnant water, which is also limited in the peatland (Sebestyen et al., 2021). While the increased mean annual air temperature and increased minimum temperature anomalies would increase *in situ* peatland MeHg production, the produced MeHg would be less likely to reach the catchment outlet due to decreased runoff from the peatland to the stream and provides a critical negative feedback limiting MeHg in our aquatic ecosystems under a warming climate.

4.3 Future Mercury Export Dynamics

Droughts and subsequent hydrological recovery are commonly linked to increased concentrations of cations, such as Hg, from peatlands (Szkokan-Emilson et al., 2013) and MeHg increases within peatlands (Coleman Wasik et al., 2015). There were several droughts (1967/68, 1976/77, 1990/91, and 2006/07) with annual precipitation < 603 mm (< 77% of the 1962-2017 mean) during the long-term record. Annual runoff ratios during drought years (0.17 ± 0.05) were significantly lower ($p = 0.04$, $t = 2.23$, $df = 10$) than the long-term mean (1962-2017, 0.22 ± 0.02), indicating that on average the entire catchment (both uplands and peatlands) was less hydrologically connected to the stream during droughts. During the 2006/07 drought, Coleman Wasik et al. (2015) observed SO_4^{2-} regeneration and subsequent elevated pore water MeHg concentrations of a nearby peatland and an increase in THg pore water concentrations after the drought. Despite increases in pore water MeHg concentrations, there was no detection of elevated annual MeHg FWC in the stream during or following the 2006/07 drought. While

droughts may promote elevated THg FWC and yields, potentially covarying with runoff ratios (Figure 2), this was not observed during the Hg record and the response was relatively limited at the annual scale. Regardless of internal Hg cycling during and after droughts, the export of Hg from peatland catchments was more dependent on the efficiency that precipitation is converted to streamwater runoff, which declines during droughts, limiting limit both MeHg and THg export under more frequent climate change induced droughts (IPCC, 2021).

Under an increasingly warming climate, MeHg production within peatlands will likely increase the pore water MeHg concentrations (Sun et al., 2023; Yang et al., 2016). However, with higher temperatures and water losses to the atmosphere, annual streamflow decreases. A resulting reduction in annual hydrological connectivity between MeHg sources and biological sinks will likely be critical in modulating aquatic MeHg concentrations under future climates. Our results using this unprecedented dataset suggest that MeHg export from headwater peatland catchments will continue to decrease over time if climate change continues to accelerate the reduction of runoff ratios and atmospheric wet Hg deposition further decreases.

5 Conclusions

Climate change and cleaner air are unequivocally altering the ecohydrological and biogeochemical processes that underpin Hg cycling and export in peatland-rich catchments. We present a clear linkage between decreasing wet Hg deposition concentration due to reductions in atmospheric Hg over North America (cleaner air) that when coupled with the climate change induced reductions in runoff ratios more than offsets the increase in MeHg production due to warmer air temperatures. Yet, the response of THg to cleaner air and climate change was much

less clear. As such, we highlight the clear need for further research into unravelling how future changes in timing and strength of hydrological connectivity within and from catchments will impact Hg export, determine the ubiquity and strength of these relationships across a greater number of catchments, and elucidate how these changes will feedback on Hg cycling in wetland and aquatic ecosystems. These critical insights would not be possible without the long-term and broad environmental measurements at the MEF. To better adapt to future climate and environmental change, there is a need for more and longer integrated multidisciplinary datasets.

Acknowledgments

We would like to thank the field and lab staff at the USDA Forest Service Northern Research Station and the University of Minnesota. We acknowledge funding provided by CPRM Canada Research Chair in Climate and Environmental Change CRC-2021-00242**.** Mention of commercial products and vendors is for informational purposes only and does not constitute endorsement, recommendation, or favor by the United States Government or the USDA Forest Service. Authors declare that they have no competing interests.

Author contributions

Conceptualization: CPRM; Methodology: CPRM, SDS, JDJ; Investigation: CPRM, SDS, JDJ, RKK, EAN; Visualization: CPRM; Funding acquisition: CPRM, JDJ, SDS; Project administration: SDS, RKK; Writing – original draft: CPRM; Writing – review & editing: CPRM, SDS, JDJ, RKK, EAN

Data Availability Statement

All data, code, and analysis are available in the main text, the supplementary materials, or referenced in Table 1. The data underlying this study are openly available in Sebestyen et al. (2022), Sebestyen et al. (2021), National Atmospheric Deposition Program (MN16) (2020), and National Atmospheric Deposition Program (MN16) (2021).

References

Åkerblom, S., Bishop, K., Björn, E., Lambertsson, L., Eriksson, T., & Nilsson, M. B. (2013). Significant interaction effects from sulfate deposition and climate on sulfur concentrations constitute major controls on methylmercury production in peatlands. *Geochimica et Cosmochimica Acta, 102*, 1-11. https://doi.org/10.1016/j.gca.2012.10.025

Barkay, T., & Gu, B. (2022). Demethylation─The Other Side of the Mercury Methylation Coin: A Critical Review. *ACS Environmental Au, 2*(2), 77-97. https://doi.org/10.1021/acsenvironau.1c00022

Bishop, K., Shanley, J. B., Riscassi, A., de Wit, H. A., Eklöf, K., Meng, B., et al. (2020). Recent advances in understanding and measurement of mercury in the environment: Terrestrial Hg cycling. *Science of The Total Environment, 721*, 137647. https://doi.org/10.1016/j.scitotenv.2020.137647

Branfireun, B. A., Cosio, C., Poulain, A. J., Riise, G., & Bravo, A. G. (2020). Mercury cycling in freshwater systems - An updated conceptual model. *Science of The Total Environment, 745*, 140906. https://doi.org/10.1016/j.scitotenv.2020.140906

Branfireun, B. a., Hilbert, D., & Roulet, N. T. (1998). Sinks and sources of methylmercury in a boreal catchment. *Biogeochemistry, 41*(3), 277-291. https://doi.org/10.1023/A:1005964603828

Chevan, A., & Sutherland, M. (1991). Hierarchical Partitioning. *The American Statistician, 45*(2), 90-96. https://doi.org/10.1080/00031305.1991.10475776

Chiasson-Gould, S. A., Blais, J. M., & Poulain, A. J. (2014). Dissolved Organic Matter Kinetically Controls Mercury Bioavailability to Bacteria. *Environmental Science & Technology, 48*(6), 3153-3161. https://doi.org/10.1021/es4038484

Coleman Wasik, J. K., Engstrom, D. R., Mitchell, C. P. J., Swain, E. B., Monson, B. A., Balogh, S. J., et al. (2015). The effects of hydrologic fluctuation and sulfate regeneration on mercury cycling in an experimental peatland. *Journal of Geophysical Research: Biogeosciences, 120*(9), 1697-1715. http://dx.doi.org/10.1002/2015JG002993

Coleman Wasik, J. K., Mitchell, C. P. J., Engstrom, D. R., Swain, E. B., Monson, B. A., Balogh, S. J., et al. (2012). Methylmercury Declines in a Boreal Peatland When Experimental Sulfate Deposition Decreases. *Environmental Science & Technology, 46*(12), 6663-6671. http://dx.doi.org/10.1021/es300865f

Demers, J. D., Driscoll, C. T., Fahey, T. J., & Yavitt, J. B. (2007). Mercury cycling in litter and soil in different forest types in the Adirondack region, New York, USA. *Ecological Applications, 17*(5), 1341-1351. https://doi.org/10.1890/06-1697.1

Deming, E. W. (1943). *Statistical adjustment of data*. New York,: John Wiley & Sons.

Dymond, S. F., Kolka, R. K., Bolstad, P. V., & Sebestyen, S. D. (2014). Long-term soil moisture patterns in a northern Minnesota forest. *Soil Science Society of America Journal, 78*(S1), S208-S216. https://doi.org/10.2136/sssaj2013.08.0322nafsc

Feng, X., Deventer, M. J., Lonchar, R., Ng, G. H. C., Sebestyen, S. D., Roman, D. T., et al. (2020). Climate Sensitivity of Peatland Methane Emissions Mediated by Seasonal Hydrologic Dynamics. *Geophysical Research Letters, 47*(17), e2020GL088875. https://doi.org/10.1029/2020GL088875

Golden, H. E., Knightes, C. D., Conrads, P. A., Feaster, T. D., Davis, G. M., Benedict, S. T., & Bradley, P. M. (2013). Climate change and watershed mercury export: a multiple projection and model analysis. *Environmental Toxicology and Chemistry, 32*(9), 2165-2174. https://doi.org/10.1002/etc.2284

Gorham, E., Eisenreich, S. J., Ford, J., & Santelmann, M. V. (1985). The chemistry of bog waters. In W. Stumm (Ed.), *Chemical processes in lakes* (pp. 339-363). New York, NY: John Wiley and Sons.

Gorski, P. R., Armstrong, D. E., Hurley, J. P., & Krabbenhoft, D. P. (2008). Influence of natural dissolved organic carbon on the bioavailability of mercury to a freshwater alga. *Environmental Pollution, 154*(1), 116-123. https://doi.org/10.1016/j.envpol.2007.12.004

Hargreaves, G. H., & Samani, Z. A. (1985). Reference Crop Evapotranspiration from Temperature. *Applied Engineering in Agriculture, 1*(2), 96-99. https://doi.org/10.13031/2013.26773

Helbig, M., Waddington, J. M., Alekseychik, P., Amiro, B. D., Aurela, M., Barr, A. G., et al. (2020). Increasing contribution of peatlands to boreal evapotranspiration in a warming climate. *Nature Climate Change, 10*(6), 555-560. https://doi.org/10.1038/s41558-020-0763-7

Helbig, M., Živković, T., Alekseychik, P., Aurela, M., El-Madany, T. S., Euskirchen, E. S., et al. (2022). Warming response of peatland CO2 sink is sensitive to seasonality in warming trends. *Nature Climate Change, 12*(8), 743-749. https://doi.org/10.1038/s41558-022-01428-z

Hintelmann, H., Harris, R., Heyes, A., Hurley, J. P., Kelly, C. A., Krabbenhoft, D. P., et al. (2002). Reactivity and mobility of new and old mercury deposition in a boreal forest ecosystem during the first year of the METAALICUS study. *Environmental Science & Technology, 36*(23), 5034-5040. https://doi.org/10.1021/es025572t

Hope, D., Billett, M. F., & Cresser, M. S. (1997). Exports of organic carbon in two river systems in NE Scotland. *Journal of Hydrology, 193*(1), 61-82. https://doi.org/10.1016/S0022-1694(96)03150-2

Hsu-Kim, H., Kucharzyk, K. H., Zhang, T., & Deshusses, M. A. (2013). Mechanisms Regulating Mercury Bioavailability for Methylating Microorganisms in the Aquatic Environment: A Critical Review. *Environmental Science & Technology, 47*(6), 2441-2456. https://doi.org/10.1021/es304370g

IPCC. (2021). *Climate Change 2021: The physical science basis. Contribution of working group I to the Sixth Assessment Report of the Intergovernmental Panel on Climate Change*. Retrieved from Geneva, Switzerland: https://www.ipcc.ch/meeting-doc/ipcc-wgi-14-and-ipcc-54/

Jeremiason, J. D., Engstrom, D. R., Swain, E. B., Nater, E. A., Johnson, B. M., Almendinger, J. E., et al. (2006). Sulfate Addition Increases Methylmercury Production in an Experimental Wetland. *Environmental Science & Technology, 40*(12), 3800-3806. http://dx.doi.org/10.1021/es0524144

Jones, M. W., Sebestyen, S. D., Dymond, S. F., Ng, G. H. C., & Feng, X. (2023). Soil frost controls streamflow generation processes in headwater catchments. *Journal of Hydrology, 617*, 128801. https://doi.org/10.1016/j.jhydrol.2022.128801

Kronberg, R.-M., Schaefer, J. K., Björn, E., & Skyllberg, U. (2018). Mechanisms of Methyl Mercury Net Degradation in Alder Swamps: The Role of Methanogens and Abiotic Processes. *Environmental Science & Technology Letters, 5*(4), 220-225. https://doi.org/10.1021/acs.estlett.8b00081

Lam, W. Y., Mackereth, R. W., & Mitchell, C. P. J. (2022). Landscape controls on total mercury and methylmercury export from small boreal forest catchments. *Biogeochemistry, 160*(1), 89-104. https://doi.org/10.1007/s10533-022-00941-9

Lee, Y. H., Bishop, K. H., Munthe, J., Iverfeldt, å., Verta, M., Parkman, H., & Hultberg, H. (1998). An examination of current Hg deposition and export in Fenno-Scandian catchments. *Biogeochemistry, 40*(2), 125-135. https://doi.org/10.1023/A:1005926321337

Li, F., Ma, C., & Zhang, P. (2020). Mercury Deposition, Climate Change and Anthropogenic Activities: A Review. *Frontiers in Earth Science, 8*. Review. https://doi.org/10.3389/feart.2020.00316

Li, L., Stewart, B., Zhi, W., Sadayappan, K., Ramesh, S., Kerins, D., et al. (2022). Climate Controls on River Chemistry. *Earth's Future, 10*(6), e2021EF002603. https://doi.org/10.1029/2021EF002603

Li, L., Sullivan, P. L., Benettin, P., Cirpka, O. A., Bishop, K., Brantley, S. L., et al. (2021). Toward catchment hydro-biogeochemical theories. *WIREs Water, 8*(1), e1495. https://doi.org/10.1002/wat2.1495

Mac Nally, R. (2000). Regression and model-building in conservation biology, biogeography and ecology: The distinction between – and reconciliation of – 'predictive' and 'explanatory' models. *Biodiversity & Conservation, 9*(5), 655-671. https://doi.org/10.1023/A:1008985925162

Mac Nally, R. (2002). Multiple regression and inference in ecology and conservation biology: further comments on identifying important predictor variables. *Biodiversity & Conservation, 11*(8), 1397-1401. https://doi.org/10.1023/A:1016250716679

McCarter, C. P. R., Branfireun, B. A., & Price, J. S. (2017). Nutrient and mercury transport in a sub-arctic ladder fen peatland subjected to simulated wastewater discharges. *Science of The Total Environment, 609*, 1349-1360. https://doi.org/10.1016/j.scitotenv.2017.07.225

McCarter, C. P. R., Eggert, S. L., Sebestyen, S. D., Kolka, R. K., & Mitchell, C. P. J. (2022a). Effects of Clearcutting and Residual Biomass Harvesting on Hillslope Mercury Mobilization and Downgradient

Mercury Accumulation. *Journal of Geophysical Research: Biogeosciences, 127*(4), e2022JG006826. https://doi.org/10.1029/2022JG006826

McCarter, C. P. R., & Price, J. S. (2017). The transport dynamics of chloride and sodium in a ladder fen during a continuous wastewater polishing experiment. *Journal of Hydrology, 549*, 558-570. http://dx.doi.org/10.1016/j.jhydrol.2017.04.033

McCarter, C. P. R., Sebestyen, S. D., Coleman Wasik, J. K., Engstrom, D. R., Kolka, R. K., Jeremiason, J. D., et al. (2022b). Long-Term Experimental Manipulation of Atmospheric Sulfate Deposition to a Peatland: Response of Methylmercury and Related Solute Export in Streamwater. *Environmental Science & Technology*. https://doi.org/10.1021/acs.est.2c02621

McCarter, C. P. R., Sebestyen, S. D., Eggert, S. L., Kolka, R. K., & Mitchell, C. P. J. (2021a). Differential subsurface mobilization of ambient mercury and isotopically enriched mercury tracers in harvested and undisturbed forests. *Biogeochemistry*. https://doi.org/10.1007/s10533-021-00801-y

Meyer-Jacob, C., Michelutti, N., Paterson, A. M., Cumming, B. F., Keller, W., & Smol, J. P. (2019). The browning and re-browning of lakes: Divergent lake-water organic carbon trends linked to acid deposition and climate change. *Scientific Reports, 9*(1), 16676. https://doi.org/10.1038/s41598-019-52912-0

Mitchell, C. P. J., Branfireun, B. A., & Kolka, R. K. (2008a). Assessing sulfate and carbon controls on net methylmercury production in peatlands: An in situ mesocosm approach. *Applied Geochemistry, 23*(3), 503-518. http://dx.doi.org/10.1016/j.apgeochem.2007.12.020

Mitchell, C. P. J., Branfireun, B. A., & Kolka, R. K. (2008b). Total mercury and methylmercury dynamics in upland–peatland watersheds during snowmelt. *Biogeochemistry, 90*(3), 225-241. https://doi.org/10.1007/s10533-008-9246-z

Mitchell, C. P. J., Branfireun, B. A., & Kolka, R. K. (2009). Methylmercury dynamics at the upland-peatland interface: Topographic and hydrogeochemical controls. *Water Resources Research, 45*(2). https://doi.org/10.1029/2008wr006832

Nathan, R. J., & McMahon, T. A. (1990). Evaluation of automated techniques for base flow and recession analyses. *Water Resources Research, 26*(7), 1465-1473. https://doi.org/10.1029/WR026i007p01465

National Atmospheric Deposition Program (MN16). (2020). National Trends Network, Site MN16. retrieved from http://nadp.slh.wisc.edu/data/sites/siteDetails.aspx?net=NTN&id=MN16

National Atmospheric Deposition Program (MN16). (2021). Mercury Deposition Network, Site MN16. retrieved from https://nadp.slh.wisc.edu/data/sites/siteDetails.aspx?net=MDN&id=MN16

O'Connor, D., Hou, D., Ok, Y. S., Mulder, J., Duan, L., Wu, Q., et al. (2019). Mercury speciation, transformation, and transportation in soils, atmospheric flux, and implications for risk management: A critical review. *Environment International, 126*, 747-761. https://doi.org/10.1016/j.envint.2019.03.019

O'Meara, M. (1998). Acid rain threats vary. In L. Brown, M. Renner, & C. Flavin (Eds.), *Vital signs the environmental trends that are shaping our future* (pp. 134-137). New York: Norton.

Pannatier, E. G., Thimonier, A., Schmitt, M., Walthert, L., & Waldner, P. (2011). A decade of monitoring at Swiss Long-Term Forest Ecosystem Research (LWF) sites: can we observe trends in atmospheric acid deposition and in soil solution acidity? *Environmental Monitoring and Assessment, 174*(1), 3-30. https://doi.org/10.1007/s10661-010-1754-3

Pierce, C. E., Furman, O. S., Nicholas, S. L., Wasik, J. C., Gionfriddo, C. M., Wymore, A. M., et al. (2022). Role of ester sulfate and organic disulfide in mercury methylation in peatland soils. *Environmental Science & Technology, 56*(2), 1433-1444. https://doi.org/10.1021/acs.est.1c04662

R Development Core Team. (2021). R: A language and environment for statistical computing (Version R 3.6.1). Vienna, Austria: R Foundation for Statistical Computing. Retrieved from http://www.R-project.org

Reshmidevi, T. V., Nagesh Kumar, D., Mehrotra, R., & Sharma, A. (2018). Estimation of the climate change impact on a catchment water balance using an ensemble of GCMs. *Journal of Hydrology, 556*, 1192-1204. https://doi.org/10.1016/j.jhydrol.2017.02.016

Schelker, J., Öhman, K., Löfgren, S., & Laudon, H. (2014). Scaling of increased dissolved organic carbon inputs by forest clear-cutting – What arrives downstream? *Journal of Hydrology, 508*, 299-306. https://doi.org/10.1016/j.jhydrol.2013.09.056

Sebestyen, S. D., Kolka, R. K., Verry, E. S., Olson, D. M., Dorrance, C., Elling, A. E., & Kyllander, R. (2011). Long-term monitoring sites and trends at the Marcell Experimental Forest. In R. K. Kolka, S. D. Sebestyen, E. S. Verry, & K. N. Brooks (Eds.), *Peatland biogeochemistry and watershed hydrology at the Marcell Experimental Forest* (pp. 15-72). Boca Raton, FL: CRC Press.

Sebestyen, S. D., & Kyllander, R. (2017). *Daily water and TOC yields for studies of the biodegradability of dissolved organic matter in peatland catchments at the Marcell Experimental Forest: 2009-2011*. https://doi.org/10.2737/RDS-2017-0068

Sebestyen, S. D., Lany, N. K., Oleheiser, K., Larson, J., Aspelin, N. A., Nelson, D. J., et al. (2022). *Marcell Experimental Forest chemistry of surface water draining the S2 catchment, 1986 - ongoing*. https://doi.org/10.6073/pasta/a47f5019f2ce2aff6cbca0e555939950

Sebestyen, S. D., Lany, N. K., Roman, D. T., Burdick, J. M., Kyllander, R. L., Verry, E. S., & Kolka, R. K. (2021). Hydrological and meteorological data from research catchments at the Marcell Experimental Forest, Minnesota, USA. *Hydrological Processes, 35*(3), e14092. https://doi.org/10.1002/hyp.14092

Sickles II, J. E., & Shadwick, D. S. (2015). Air quality and atmospheric deposition in the eastern US: 20 years of change. *Atmospheric Chemistry and Physics, 15*(1), 173-197. https://doi.org/10.5194/acp-15-173-2015

Skyllberg, U. (2008). Competition among thiols and inorganic sulfides and polysulfides for Hg and MeHg in wetland soils and sediments under suboxic conditions: Illumination of controversies and implications for MeHg net production. *Journal of Geophysical Research: Biogeosciences, 113*(G2). https://doi.org/10.1029/2008jg000745

Skyllberg, U., Qian, J., Frech, W., Xia, K., & Bleam, W. F. (2003). Distribution of mercury, methyl mercury and organic sulphur species in soil, soil solution and stream of a boreal forest catchment. *Biogeochemistry, 64*(1), 53-76. journal article. https://doi.org/10.1023/a:1024904502633

Sonke, J. E., Angot, H., Zhang, Y., Poulain, A., Björn, E., & Schartup, A. (2023). Global change effects on biogeochemical mercury cycling. *AMBIO, 52*(5), 853-876. https://doi.org/10.1007/s13280-023-01855-y

Sun, T., Lindo, Z., & Branfireun, B. A. (2023). Ground warming releases inorganic mercury and increases net methylmercury production in two boreal peatland types. *Frontiers in Environmental Science, 11*. Original Research. https://doi.org/10.3389/fenvs.2023.1100443

Szkokan-Emilson, E. J., Kielstra, B., Watmough, S., & Gunn, J. (2013). Drought-induced release of metals from peatlands in watersheds recovering from historical metal and sulphur deposition. *Biogeochemistry, 116*(1-3), 131-145. Article. http://dx.doi.org/10.1007/s10533-013-9919-0

Tjerngren, I., Karlsson, T., Bj, xf, rn, E., & Skyllberg, U. (2012a). Potential Hg methylation and MeHg demethylation rates related to the nutrient status of different boreal wetlands. *Biogeochemistry, 108*(1/3), 335-350.

Tjerngren, I., Meili, M., Björn, E., & Skyllberg, U. (2012b). Eight Boreal Wetlands as Sources and Sinks for Methyl Mercury in Relation to Soil Acidity, C/N Ratio, and Small-Scale Flooding. *Environmental Science & Technology, 46*(15), 8052-8060. https://doi.org/10.1021/es300845x

Urban, N. R., Eisenreich, S. J., & Grigal, D. F. (1989). Sulfur cycling in a forested Sphagnum bog in northern Minnesota. *Biogeochemistry, 7*(2), 81-109. journal article. https://doi.org/10.1007/bf00004123

Verry, E. S., Brooks, K. N., Nicholas, D. S., Ferris, D. R., & Sebestyen, S. D. (2011). Watershed Hydrology. In R. K. Kolka, S. Sebestyen, E. S. Verry, & K. Brooks (Eds.), *Peatland biogeochemistry and watershed hydrology at the Marcell Experimental Forest* (pp. 193-212). Boca Raton, FL: CRC Press.

Verry, E. S., Elling, A. E., Sebestyen, S. D., Kolka, R. K., & Kyllander, R. (2018). *Marcell Experimental Forest daily streamflow data*. https://doi.org/10.2737/RDS-2018-0009

Verry, E. S., & Janssens, J. (2011). Geology, vegetation, and hydrology of the S2 bog at the MEF: 12,000 years in northern Minnesota. In R. K. S. Kolka, Stephen D.; Verry, Elon S.; Brooks,Kenneth N. (Ed.), *Peatland biogeochemistry and watershed hydrology at the Marcell Experimental Forest* (pp. 93-134). Boca Raton, FL.: CRC Press.

Walsh, C., & Mac Nally, R. (2020). Hierarchical Partitioning (Version 1.0-6): CRAN. Retrieved from https://cran.r-project.org/web/packages/hier.part/index.html

Wei, T., & Simko, V. (2017). R package "corrplot": Visualization of a Correlation Matrix (Version Version 0.84). Retrieved from https://github.com/taiyun/corrplot

Woerndle, G. E., Tsz-Ki Tsui, M., Sebestyen, S. D., Blum, J. D., Nie, X., & Kolka, R. K. (2018). New insights on ecosystem mercury cycling revealed by stable isotopes of mercury in water flowing from a headwater peatland catchment. *Environmental Science & Technology, 52*(4), 1854-1861. https://doi.org/10.1021/acs.est.7b04449

Wu, C., & Yu, J. Z. (2018). Evaluation of linear regression techniques for atmospheric applications: the importance of appropriate weighting. *Atmos. Meas. Tech., 11*(2), 1233-1250. https://doi.org/10.5194/amt-11-1233-2018

Yang, Z., Fang, W., Lu, X., Sheng, G.-P., Graham, D. E., Liang, L., et al. (2016). Warming increases methylmercury production in an Arctic soil. *Environmental Pollution, 214*, 504-509. https://doi.org/10.1016/j.envpol.2016.04.069

York, D. (1966). Least-squares fitting of a straight line. *Canadian Journal of Physics, 44*(5), 1079-1086. https://doi.org/10.1139/p66-090

Zhang, L., Zhou, P., Cao, S., & Zhao, Y. (2019). Atmospheric mercury deposition over the land surfaces and the associated uncertainties in observations and simulations: a critical review. *Atmos. Chem. Phys., 19*(24), 15587-15608. https://doi/org/10.5194/acp-19-15587-2019

Zhang, Y., Zheng, H., Zhang, X., Leung, L. R., Liu, C., Zheng, C., et al. (2023). Future global streamflow declines are probably more severe than previously estimated. *Nature Water*. https://doi.org/10.1038/s44221-023-00030-7

673 **Figure Captions**
674
675 Figure 1. Annual THg and MeHg flow-weighted concentrations (FWC) and %MeHg from 2001
676 through 2017 at the S2 catchment in the USDA Forest Service Marcell Experimental Forest.
677 Linear regression (solid lines) and 95% confidence intervals illustrate the average temporal
678 trends. Note the gap in the MeHg record due to a resolved analytical contamination issue
679 (McCarter et al., 2022b).
680
681 Figure 2. Error-in-variable linear regressions using Deming Regression (solid line) between
682 annual flow-weighted MeHg concentration and the annual average air temperature, annual
683 average wet Hg deposition concentration, and annual runoff ratio. Dashed lines represent the
684 95% confidence interval.
685
686 Figure 3. Annual THg (**A**) and MeHg (**B**) yields from 2001 through 2017 at the S2 catchment in
687 the USDA Forest Service Marcell Experimental Forest.
688
689 Figure 4. Annual total and concentration of wet Hg deposition, and the annual average
690 precipitation pH and SO_4^{2-} concentration from 1980 through 2017 (Hg: 1995 – 2017) at the
691 USDA Forest Service Marcell Experimental Forest.
692
693 Figure 5. The change in annual average air temperature (**A**), total precipitation (**B**), streamflow
694 (**C**), and runoff ratio (**D**) from 1962 through 2017 at the USDA Forest Service Marcell
695 Experimental Forest. Solid lines are the LOESS smoothed lines resulting from the Mann-Kendall
696 trend tests.
697

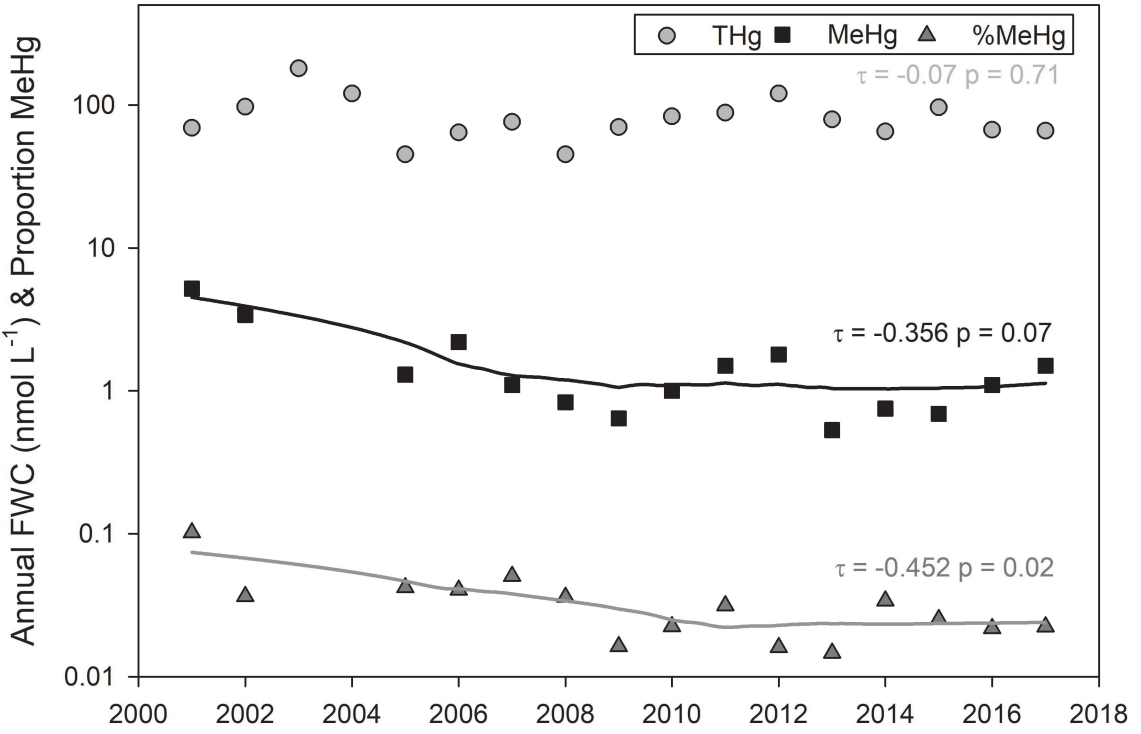
THg
MeHg
%MeHg
τ = -0.07 p = 0.71
τ = -0.356 p = 0.07
τ = -0.452 p = 0.02
Annual FWC (nmol L-1) & Proportion MeHg
100
10
1
0.1
0.01
2000
2002
2004
2006
2008
2010
2012
2014
2016
2018

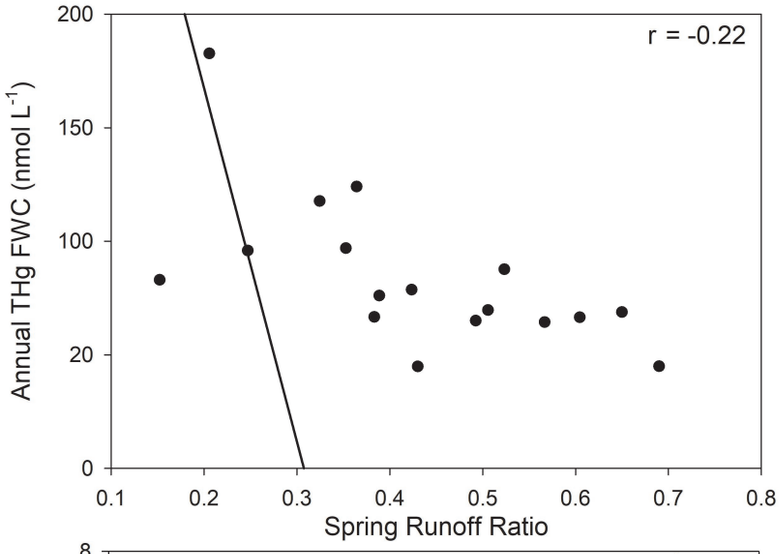
r = -0.22
Annual THg FWC (nmol L-1)
Spring Runoff Ratio

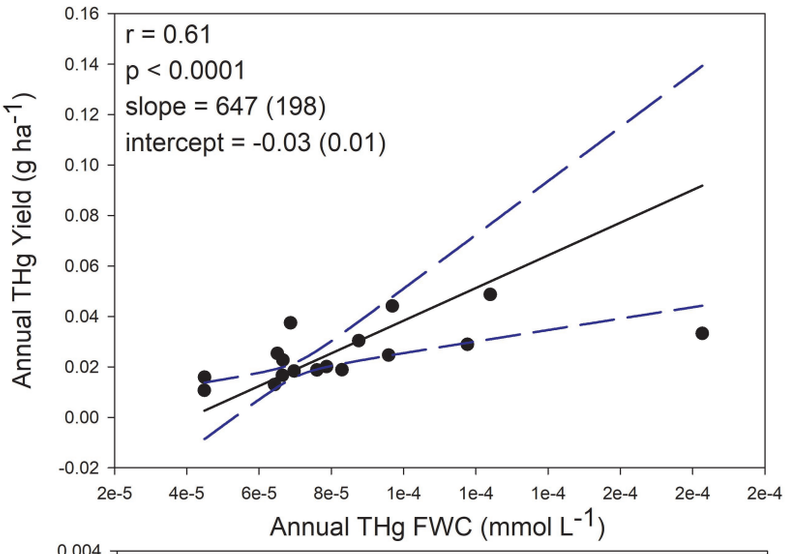
r = 0.61
p < 0.0001
slope = 647 (198)
intercept = -0.03 (0.01)
Annual THg Yield (g ha-1)
Annual THg FWC (mmol L-1)

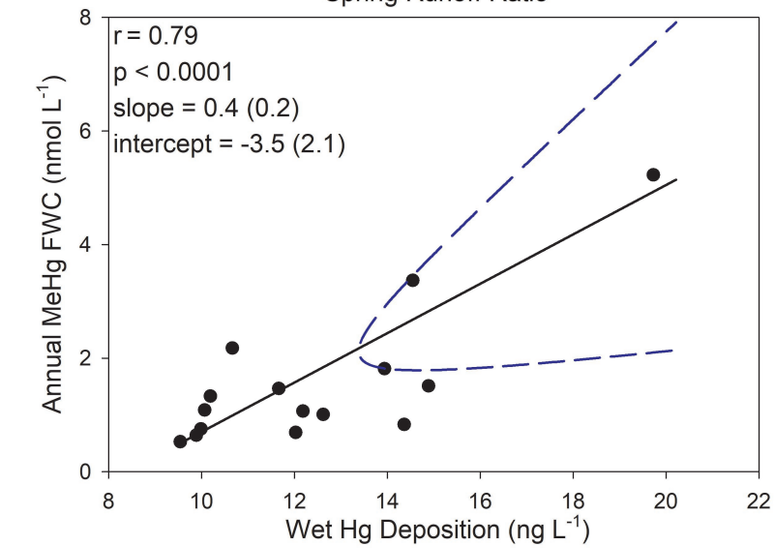
r = 0.79
p < 0.0001
slope = 0.4 (0.2)
intercept = -3.5 (2.1)
Annual MeHg FWC (nmol L-1)
Wet Hg Deposition (ng L-1)

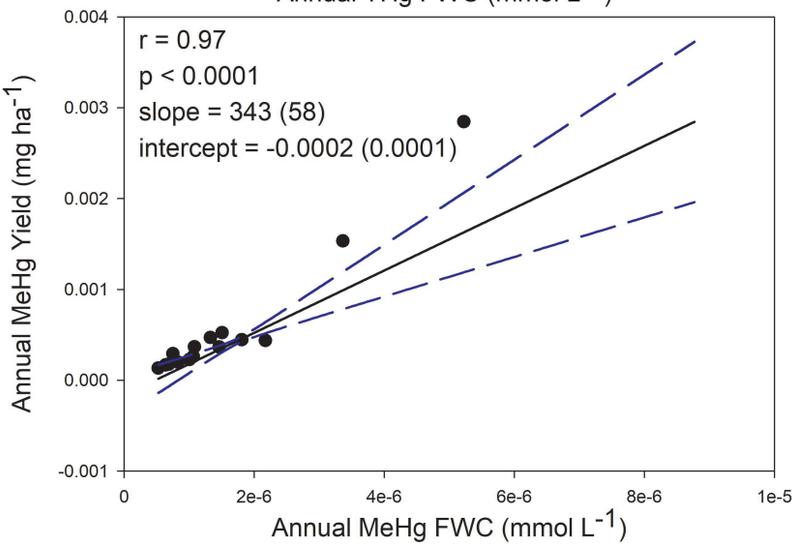
r = 0.97
p < 0.0001
slope = 343 (58)
intercept = -0.0002 (0.0001)
Annual MeHg Yield (mg ha-1)
Annual MeHg FWC (mmol L-1)

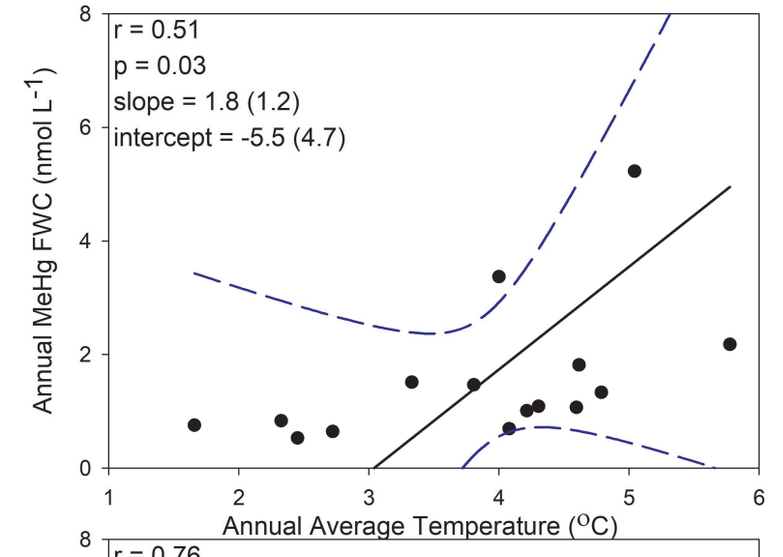
r = 0.51
p = 0.03
slope = 1.8 (1.2)
intercept = -5.5 (4.7)
Annual MeHg FWC (nmol L-1)
Annual Average Temperature (OC)

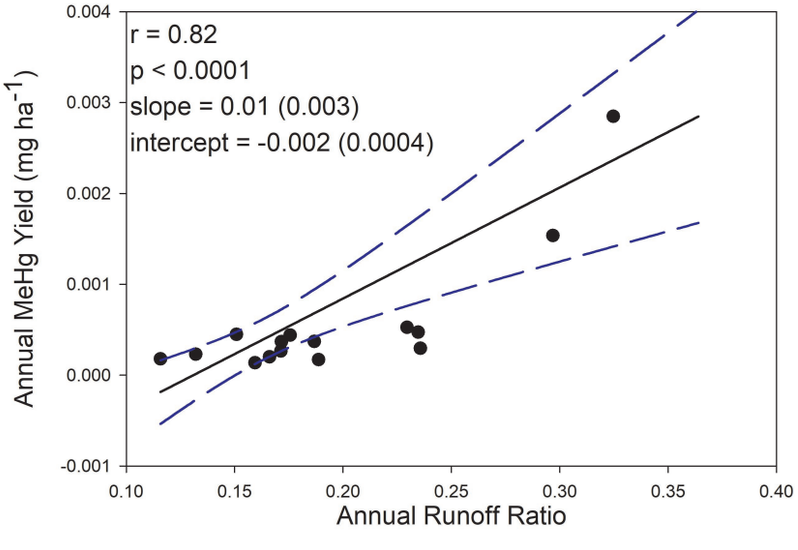
r = 0.82
p < 0.0001
slope = 0.01 (0.003)
intercept = -0.002 (0.0004)
Annual MeHg Yield (mg ha-1)
Annual Runoff Ratio

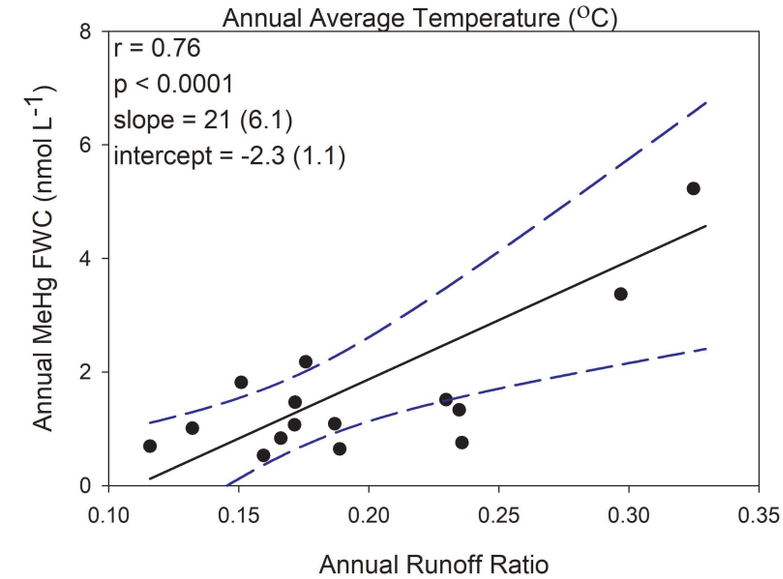
r = 0.76
p < 0.0001
slope = 21 (6.1)
intercept = -2.3 (1.1)
Annual MeHg FWC (nmol L-1)
Annual Runoff Ratio

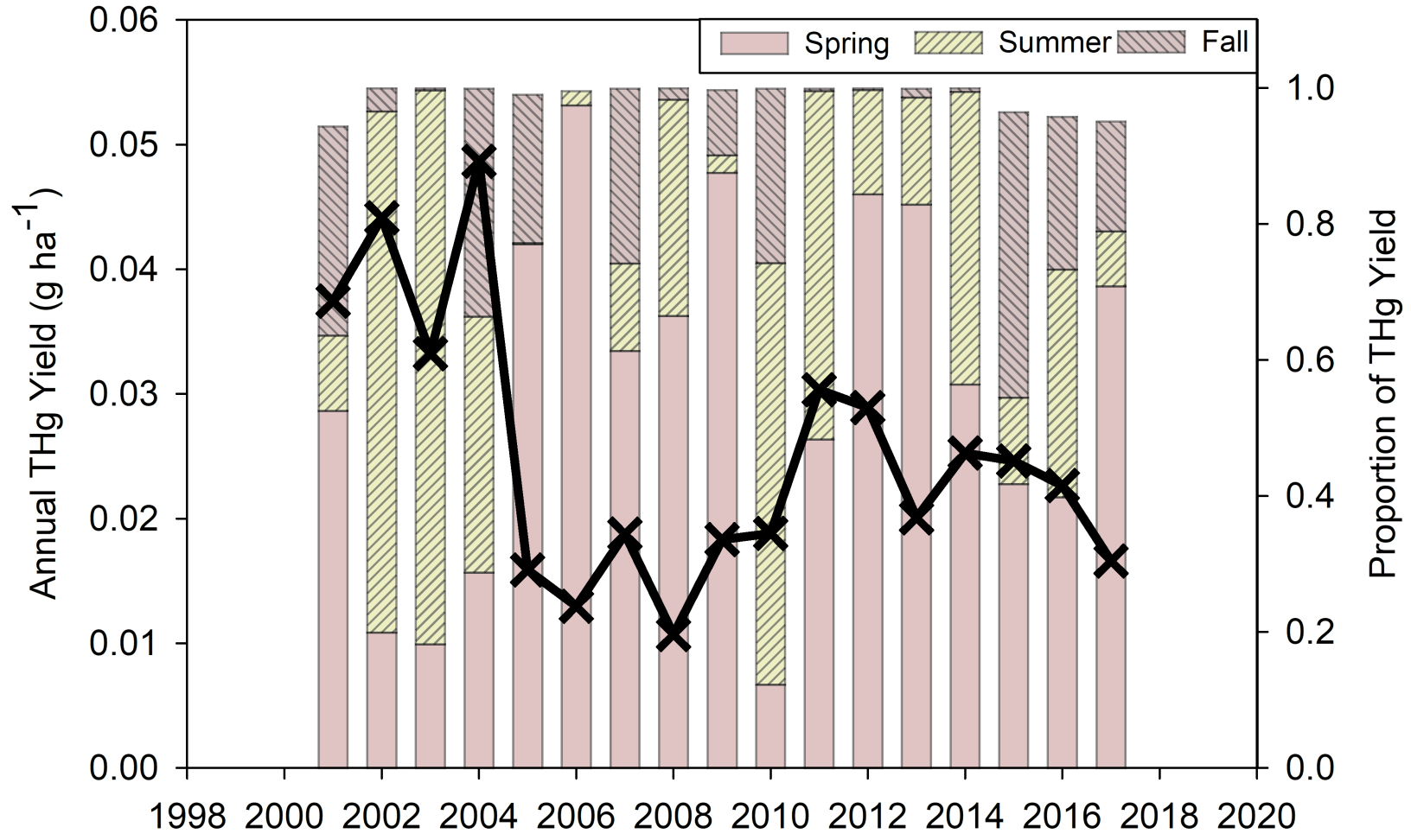
Spring
Summer
Fall
Annual THg Yield (g ha-1)
Proportion of THg Yield
0.00
0.01
0.02
0.03
0.04
0.05
0.06
0.0
0.2
0.4
0.6
0.8
1.0
1998
2000
2002
2004
2006
2008
2010
2012
2014
2016
2018
2020

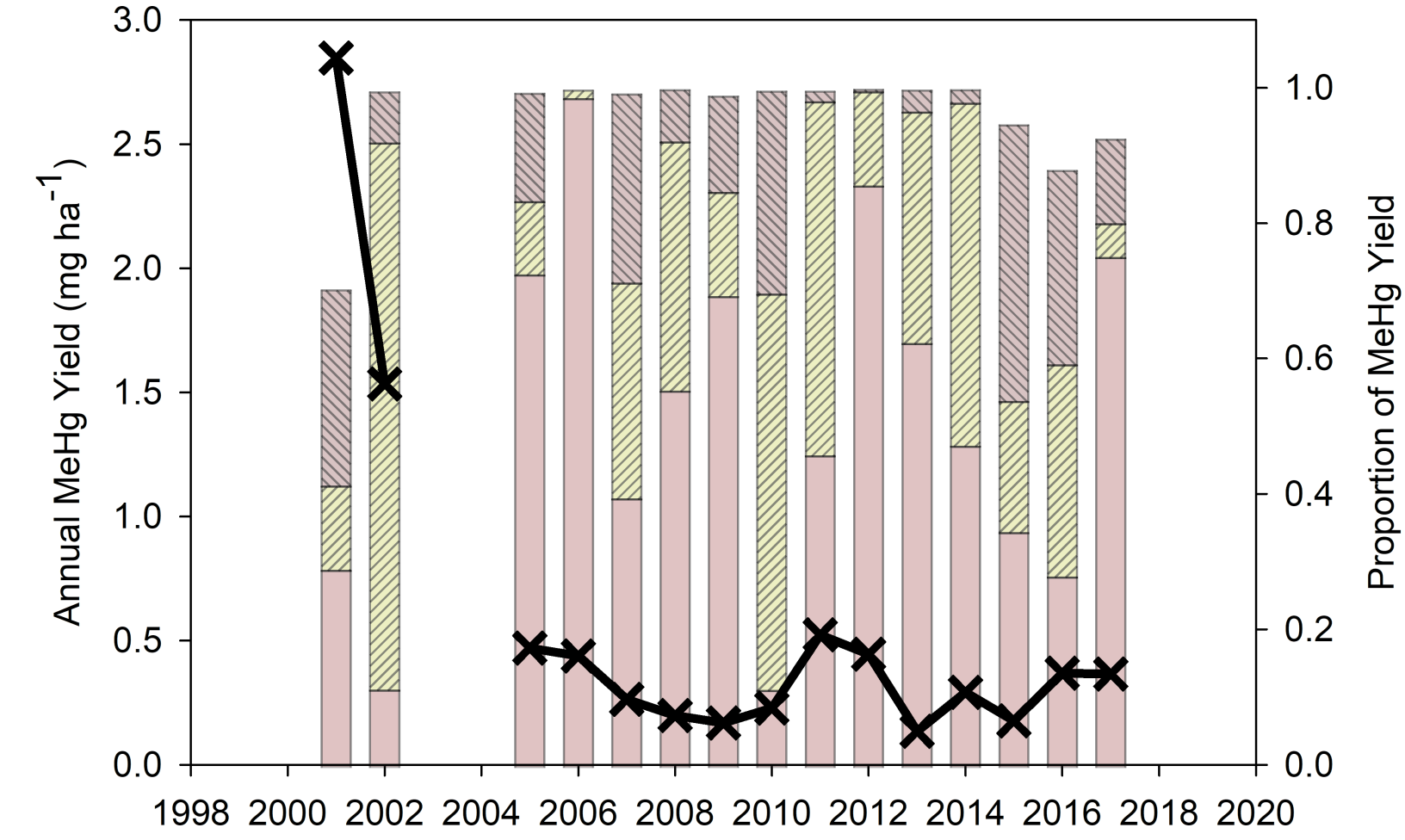
Annual MeHg Yield (mg ha-1)
Proportion of MeHg Yield
0.0
0.5
1.0
1.5
2.0
2.5
3.0
0.0
0.2
0.4
0.6
0.8
1.0
1998
2000
2002
2004
2006
2008
2010
2012
2014
2016
2018
2020

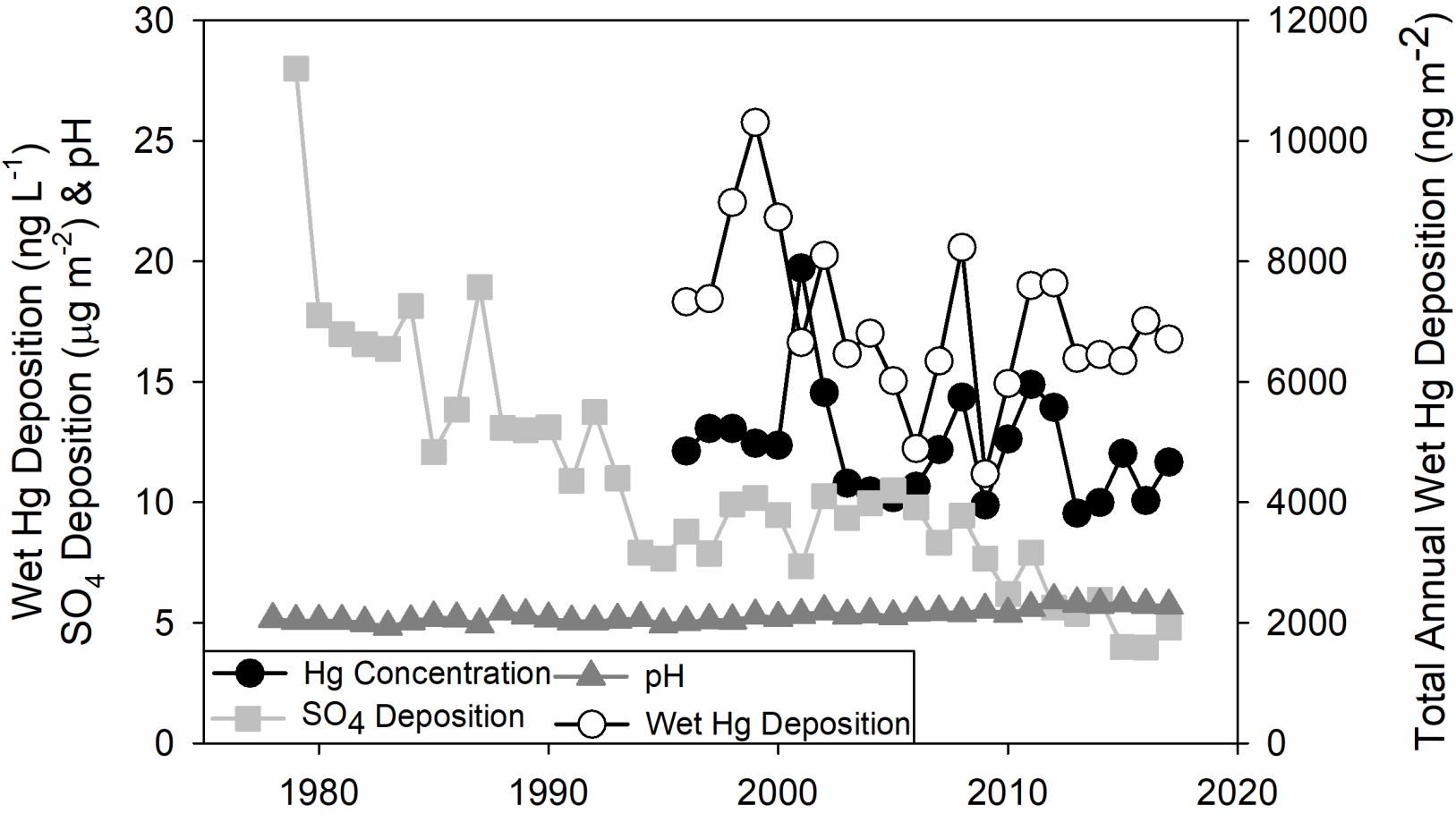
Wet Hg Deposition (ng L-1)
SO4 Deposition (µg m-2) & pH
Total Annual Wet Hg Deposition (ng m-2)
30
25
20
15
10
5
0
12000
10000
8000
6000
4000
2000
0
1980
1990
2000
2010
2020
Hg Concentration
pH
SO4 Deposition
Wet Hg Deposition

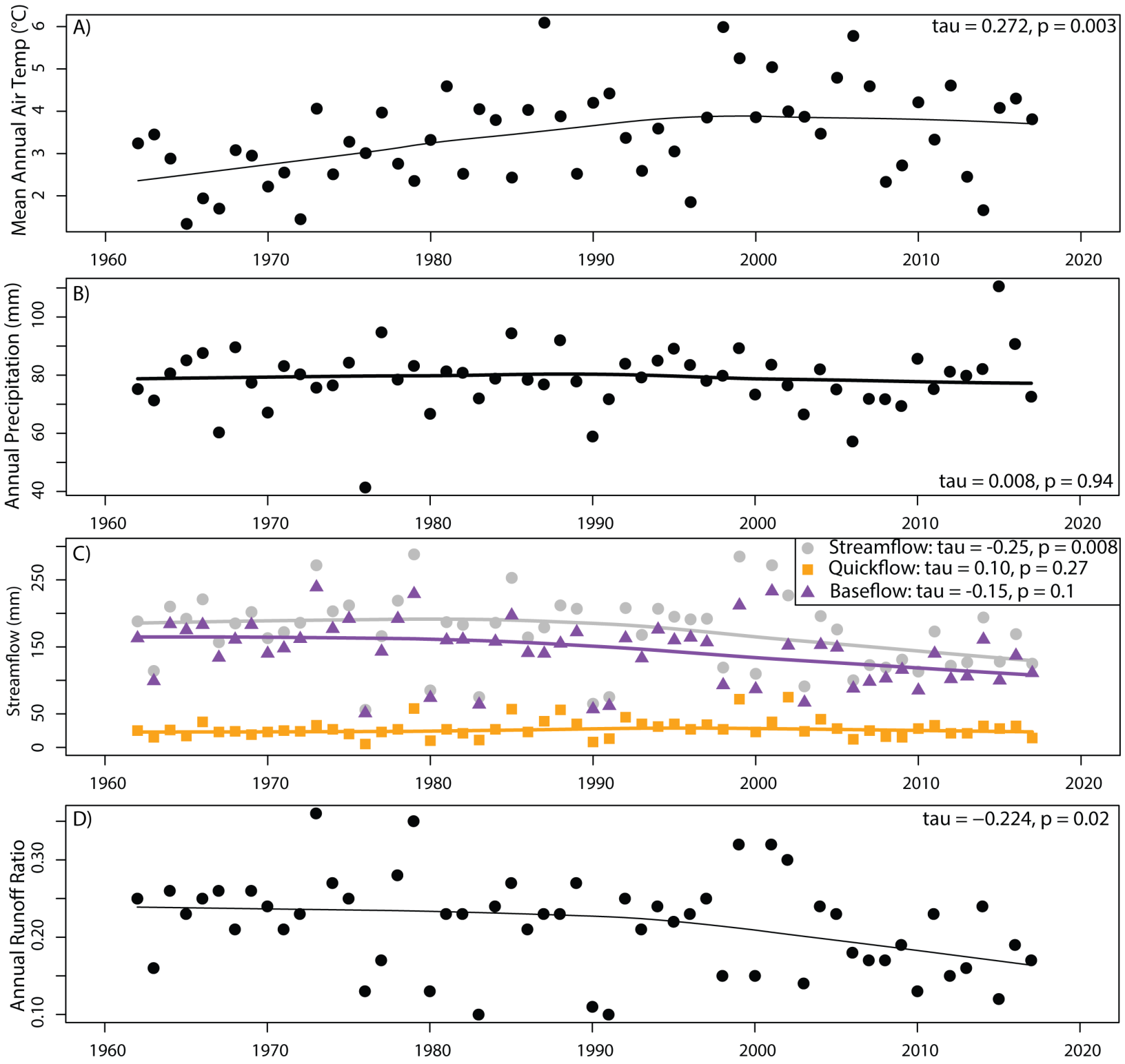
A)
tau = 0.272, p = 0.003
Mean Annual Air Temp (°C)
2
3
4
5
6
1960
1970
1980
1990
2000
2010
2020
B)
Annual Precipitation (mm)
40
60
80
100
tau = 0.008, p = 0.94
C)
Streamflow: tau = -0.25, p = 0.008
Quickflow: tau = 0.10, p = 0.27
Baseflow: tau = -0.15, p = 0.1
Streamflow (mm)
0
50
150
250
D)
tau = −0.224, p = 0.02
Annual Runoff Ratio
0.10
0.20
0.30

AGU Advances

Supporting Information for

Climate change and cleaner emissions decrease methylmercury export from a headwater peatland catchment

C.P.R. McCarter[1], S.D. Sebestyen[2], J.D. Jeremiason[3], E.A. Nater[4], R.K. Kolka[2]

[1] Department of Biology and Chemistry & Department of Geography, Nipissing University; 100 College Drive, North Bay, Ontario, Canada

[2] USDA Forest Service Northern Research Station, Grand Rapids, Minnesota 55744, USA

[3] Department of Chemistry, Gustavus Adolphus College, 800 W College Ave St. Peter, MN 56082, USA

[4] Department of Soil, Water, and Climate, University of Minnesota, St. Paul, Minnesota 55108, USA

Contents of this file

Introduction

In this supplement, we provide supplemental figures and tables that enhance the main manuscript. This document includes two sections: Supplementary Figures and Supplementary Tables. The Supplementary Figures section contains the hierarchal clustered Pearson correlation matrix, changes in seasonal runoff ratios, and changes in annual proportion event flow. The Supplementary Tables sections contains the mean (± one standard deviation) annual flow-weighted concentrations (FWC) for total mercury (THg) and methylmercury (MeHg), mean (± one standard deviation) annual temperature, annual and spring runoff ratios, and mean (± one standard deviation) wet mercury (Hg) deposition concentration, as well as the independent and joint variability for all hierarchal partitioning regressions. Note, there is a two year gap in the MeHg concentration data due to a now resolved laboratory contamination issue. For more detail of this issue see McCarter et al. (2022) and Sebestyen et al. (2022).

Supplementary Figures

Figure S1. The hierarchal clustered Pearson correlation matrix. Larger circles indicate smaller p-values, while no circle indicate p > 0.05. Note, a higher resolution of Figure S1 is provided as an additional supplementary file.

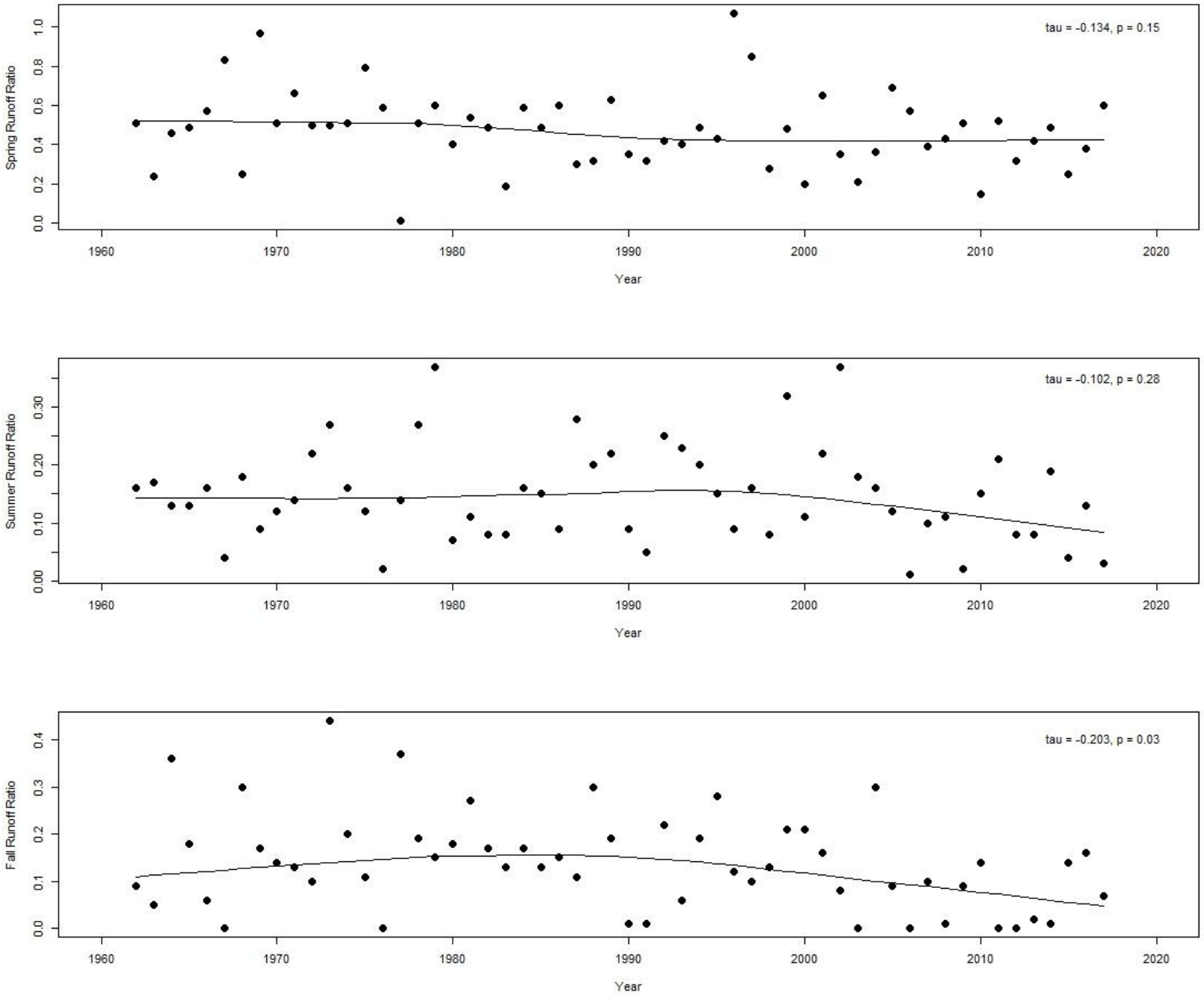

Figure S2. Changes in seasonal runoff ratios 1962 through 2017 at the USDA Forest Service Marcell Experimental Forest. Solid lines are the LOESS smoothed lines resulting from the Mann-Kendall trend tests.

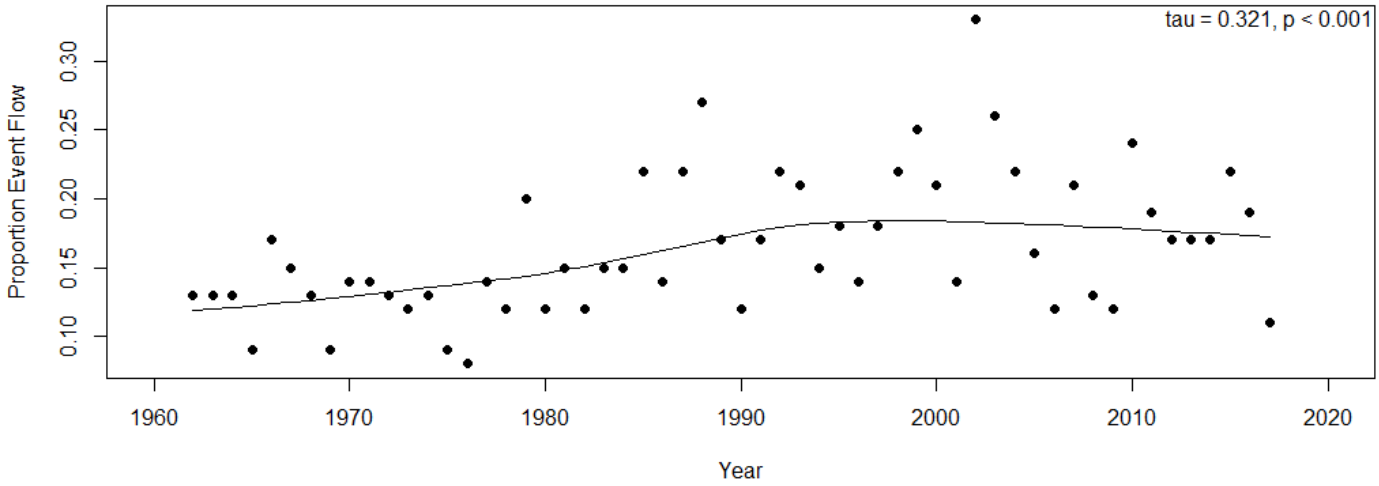

Figure S3. The change in annual event flow from 1962 through 2017 at the USDA Forest Service Marcell Experimental Forest. Solid lines are the LOESS smoothed lines resulting from the Mann-Kendall trend tests.

Supplemental Tables

Table S1. The FWC and yields (± one standard deviation) of THg and MeHg, as well as mean (± one standard deviation) of mean annual air temperature, annual runoff ratio, mean annual wet Hg deposition concentration, and spring runoff ratio.

Year	THg FWC	THg Yield	MeHg FWC	MeHg Yield	Mean Annual Air Temperature	Annual Runoff Ratio	Mean Wet Hg Deposition Concentration	Spring Runoff Ratio
	nmol L^{-1}	g ha^{-1}	nmol L^{-1}	mg ha^{-1}	°C	-	ng L^{-1}	-
2001	68.8 ± 16.4	0.04 ± 0.0017	5.2 ± 15.6	2.8 ± 0.078	5 ± 12.1	0.32 ± 0.29	19.7 ± 9.3	0.65 ± 0.45
2002	96.9 ± 24	0.04 ± 0.0023	3.4 ± 5.4	1.5 ± 0.001	4 ± 12.3	0.3 ± 0.28	14.5 ± 13.3	0.35 ± 0.45
2003	182.7 ± 35.4	0.03 ± 0.0022	-	-	3.9 ± 12.3	0.14 ± 0.01	10.8 ± 13.3	0.21 ± 0.13
2004	124 ± 22.1	0.05 ± 0.00199	-	-	3.5 ± 13.4	0.24 ± 0.29	10.5 ± 8.8	0.36 ± 0.78
2005	44.9 ± 9.5	0.02 ± 0.0008	1.3 ± 1.7	0.5 ± 0.001	4.8 ± 12.9	0.23 ± 1	10.2 ± 6.8	0.69 ± 2.01
2006	64.3 ± 5.6	0.01 ± 0.0004	2.2 ± 7.7	0.4 ± 0.002	5.8 ± 11.5	0.18 ± 0.59	10.7 ± 8.5	0.57 ± 1.09
2007	76 ± 6.6	0.02 ± 0.0005	1.1 ± 9	0.3 ± 0.002	4.6 ± 13.4	0.17 ± 0.25	12.2 ± 11.7	0.39 ± 0.41
2008	44.8 ± 6.1	0.01 ± 0.0004	0.8 ± 3.8	0.2 ± 0.0002	2.3 ± 13.4	0.17 ± 0.19	14.4 ± 24	0.43 ± 0.3
2009	69.7 ± 2.1	0.02 ± 0.0002	0.6 ± 1.5	0.2 ± 0.00001	2.7 ± 12.8	0.19 ± 0.46	9.9 ± 15.3	0.51 ± 0.76
2010	83 ± 5.3	0.02 ± 0.0004	1 ± 5.3	0.2 ± 0.0001	4.2 ± 12.5	0.13 ± 0.08	12.6 ± 17.4	0.15 ± 0.07
2011	87.6 ± 6.7	0.03 ± 0.0006	1.5 ± 3.3	0.5 ± 0.0001	3.3 ± 12.7	0.23 ± 0.2	14.9 ± 14.8	0.52 ± 0.31
2012	117.7 ± 62.7	0.03 ± 0.0045	1.8 ± 0.2	0.4 ± 0.00005	4.6 ± 12	0.15 ± 0.15	13.9 ± 14.9	0.32 ± 0.12
2013	78.7 ± 4.8	0.02 ± 0.0003	0.5 ± 2	0.1 ± 0.0004	2.5 ± 13.9	0.16 ± 0.32	9.5 ± 8.6	0.42 ± 0.6
2014	65.1 ± 10.9	0.03 ± 0.00097	0.8 ± 2.7	0.3 ± 0.0002	1.7 ± 14.1	0.24 ± 0.24	10 ± 8.1	0.49 ± 0.37
2015	95.9 ± 15.8	0.02 ± 0.0012	0.7 ± 3.1	0.2 ± 0.0002	4.1 ± 12.8	0.12 ± 0.12	12 ± 12.4	0.25 ± 0.17
2016	66.6 ± 4.2	0.02 ± 0.0004	1.1 ± 3.3	0.4 ± 0.0004	4.3 ± 12.3	0.19 ± 0.17	10.1 ± 9.5	0.38 ± 0.26
2017	66.5 ± 12.2	0.02 ± 0.0009	1.5 ± 1.3	0.4 ± 0.00005	3.8 ± 12.6	0.17 ± 0.28	11.7 ± 11.3	0.6 ± 0.34

Table S2. The independent and joint variability explained by each driver of THg FWC from the hierarchal partitioning regression and Z scores. **Bold** and *italic* indicate significant at $p < 0.05$.

Driver	Independent Variability	Joint Variability	Total Variability	% Independent Variability	Z score
Annual Precipitation pH	-0.005	0.003	-0.002	3	-0.580
Spring Runoff Ratio	-0.134	-0.017	-0.151	89	***4.370***
Summer Precipitation pH	-0.012	-0.004	-0.016	8	-0.350

Table S3. The independent and joint variability explained by each driver of THg yields from the hierarchal partitioning regression and Z scores. **Bold** and *italic* indicate significant at $p < 0.05$.

Driver	Independent Variability	Joint Variability	Total Variability	% Independent Variability	Z score
Annual Streamflow	-0.02	0.015	-0.01	4	-0.05
Annual Event Flow	-0.02	-0.006	-0.02	3	-0.23
Summer Streamflow	-0.01	-0.010	-0.02	2	-0.34
Summer Proportion Event Flow	-0.02	-0.029	-0.04	3	-0.25
Summer Runoff Ratio	-0.02	-0.002	-0.02	3	-0.19
THg FWC	-0.42	-0.044	-0.46	84	***14.12***

Table S4. The independent and joint variability explained by each driver of MeHg FWC from the hierarchal partitioning regression and Z scores. **Bold** and *italic* indicate significant at $p < 0.05$.

Driver	Independent Variability	Joint Variability	Total Variability	% Independent Variability	Z score
Baseflow	-0.07	-0.11	-0.18	9.6	0.54
Runoff Ratio	-0.15	-0.12	-0.27	20.4	***2.25***
Annual Avg. Temp	-0.17	-0.07	-0.24	22.8	***2.65***
Summer Avg. Temp	-0.10	-0.16	-0.26	12.7	1.05
10yr avg. PET	-0.08	-0.19	-0.27	10.7	0.85
Wet Hg Deposition Concentration	-0.18	-0.14	-0.32	23.8	***2.58***

Table S5. The independent and joint variability explained by each driver of MeHg Yield from the hierarchal partitioning regression and Z scores. Bold and *italic* indicate significant at $p < 0.05$.

Driver	Independent Variability	Joint Variability	Total Variability	% Independent Variability	Z score
Streamflow	-0.13	-0.36	-0.50	12.1	1.07
Runoff Ratio	-0.18	-0.36	-0.53	16.2	***1.82***
Annual Avg. Temp	-0.10	-0.07	-0.17	9.1	0.73
Event Flow	-0.11	-0.19	-0.30	10.1	0.57
10yr avg. PET	-0.10	-0.30	-0.40	8.8	0.70
Wet Hg Deposition Concentration	-0.12	-0.29	-0.41	11.5	0.87
MeHg FWC	-0.35	-0.57	-0.92	32.2	***3.96***

References

McCarter, C. P. R., Sebestyen, S. D., Coleman Wasik, J. K., Engstrom, D. R., Kolka, R. K., Jeremiason, J. D., et al. (2022). Long-Term Experimental Manipulation of Atmospheric Sulfate Deposition to a Peatland: Response of Methylmercury and Related Solute Export in Streamwater. *Environmental Science & Technology*. https://doi.org/10.1021/acs.est.2c02621

Sebestyen, S. D., Lany, N. K., Oleheiser, K., Larson, J., Aspelin, N. A., Nelson, D. J., et al. (2022). *Marcell Experimental Forest chemistry of surface water draining the S6 catchment, 1986 - ongoing*. https://doi.org/10.6073/pasta/9f8fb5bb7ce3d9549e2cab219fdc65d8